

BBN bounds on active-sterile neutrino mixing

A.D. Dolgov^{(a)(b)(c)(d)} and F.L. Villante^{(a)(d)}

^(a) *INFN, sezione di Ferrara, Via Paradiso, 12 - 44100 Ferrara, Italy*

^(b) *ITEP, Bol. Chermushkinskaya 25, Moscow 113259, Russia*

^(c) *Research Center for the Early Universe, Graduate School of Science,
University of Tokyo, Tokyo 113-0033, Japan*

^(d) *Dipartimento di Fisica, Universita' di Ferrara, Via Paradiso 12 - 44100 Ferrara, Italy*

Abstract

Nucleosynthesis restrictions on mixing of active neutrinos with possible sterile ones are obtained with the account of experimentally determined mixing between all active neutrinos. The earlier derived bounds, valid in the absence of active-active mixing, are reanalyzed and significant difference is found in the resonance case. The results are obtained both analytically and numerically by solution of complete system of integro-differential kinetic equations. A good agreement between analytical and numerical approaches is demonstrated. A role of possibly large cosmological lepton asymmetry is discussed.

1 Introduction

Combined data from SNO [1], KamLAND [2], and earlier data on solar [3] and atmospheric [4] neutrino deficit present strong indication that all these neutrino anomalies can be explained without introduction of a new sterile neutrino, for recent analysis see refs. [5]-[11]). According to ref. [8], a mixing of active, ν_a ($a = e, \mu, \tau$), and sterile, ν_s , neutrinos is excluded at the level $\sin \eta < 0.13$. On the other hand, at a weaker level, mixing with ν_s is not only allowed but even desirable. According the ref. [12], some features of the solar neutrino data are better described if there exists fourth sterile neutrino state with the mixing parameter $\sin^2 2\theta = 10^{-4} - 10^{-3}$ and the mass difference $\delta m^2 = (10^{-5} - 10^{-6})$ eV². Moreover, the LSND results [13] probably also demands mixing with additional one or several new (sterile) neutrinos or maybe, if confirmed, something even more drastic.

Consideration of big bang nucleosynthesis (BBN) may noticeably strengthen the upper bound on mixing between active and sterile neutrinos and even exclude explanation of LSND anomaly by admixture of ν_s . Such limits can also restrict explanations of solar and atmospheric neutrino features by an admixture of ν_s . BBN bounds on mixing between ν_s and ν_a were derived long time ago [14]-[19] under assumption that only one active neutrino is mixed with a sterile partner and mixing between active neutrinos was disregarded (for more references and discussion see the review [20]). A simplified consideration of 4 neutrino mixing has been done recently in ref. [21] for rather large mixing angle, $\sin^2 2\theta_{as} > 0.01$.

It is practically established now that all active neutrinos, ν_e , ν_μ , and ν_τ , are strongly mixed with the parameters given by Large Mixing Angle (LMA) solution to solar neutrino deficit [11]:

$$\delta m_{\text{sol}}^2 = 7.3 \cdot 10^{-5} \text{ eV}^2, \quad \tan^2 \theta_{\text{sol}} = 0.4 \quad (1)$$

and by atmospheric neutrino data [4]:

$$\delta m_{\text{atmo}}^2 = 2.5 \cdot 10^{-3} \text{ eV}^2, \quad \tan^2 \theta_{\text{atmo}} \approx 1 \quad (2)$$

Existence of fast transitions between ν_e , ν_μ , and ν_τ noticeably changes BBN bound on mixing with sterile neutrinos especially for small values of mass difference. The reason for this change is the following. There are three possible effects on BBN created by mixing between active and sterile neutrinos. First is the production of additional neutrino species in the primeval plasma. The second effect is a depletion of the number density of electronic neutrinos which results in a higher neutron freezing temperature. Both these effects lead to a larger neutron-to-proton ratio and to more abundant production of primordial deuterium and helium-4 (for the details see e.g. review [20]). If mixing between active neutrinos is absent then the second effect would manifest itself only in the case of $(\nu_e - \nu_s)$ -mixing, if we neglect relatively weak depopulation of ν_e through the annihilation $\bar{\nu}_e \nu_e \rightarrow \bar{\nu}_{\mu,\tau} \nu_{\mu,\tau}$. In the realistic case of experimentally measured mixing between all active neutrinos a deficit of ν_μ or ν_τ would be efficiently transformed into deficit of ν_e leading to a stronger BBN bound on active-sterile mixing.

The third effect is a generation of large lepton asymmetry due to oscillations between active and sterile species [22]. However, this effect takes place only for very weak mixing, much smaller than the experimental bound and is neglected throughout almost all the paper, except for sec. 7.

The paper is organized as follows. In sec. 2 general kinetic equations for oscillating neutrinos in the primeval cosmological plasma are presented. In sec. 3 the approximations that we use for analytical and numerical calculations are discussed and the effects of neutrino on Big Band Nucleosynthesis (BBN) are described. In sec. 4 we reconsider the case of mixing between one active and one sterile neutrinos, assuming that other active neutrinos are not mixed. Our calculations agree with the earlier works in non-resonance case, while there is a noticeable difference in the resonance case. In sec 5 we consider for illustrative purposes algebraically much simpler situation when only two active neutrinos are mixed. The realistic case of all three active neutrinos mixed is presented in sec. 6. In all previous sections the calculations are done for negligibly small cosmological lepton asymmetry. The impact of the latter is discussed in sec. 7. In conclusion we summarize and discuss the derived bounds.

2 Kinetic equations

We assume that in addition to three known active neutrinos there exists a fourth neutrino flavor which does not have any interactions except for mixing with active neutrinos. The transformation between flavor eigenstates ν_α and mass eigenstates ν_j is described by the orthogonal matrix

$$\nu_\alpha = U_{\alpha j} \nu_j \quad (3)$$

where $\alpha = e, \mu, \tau, s$ and $j = 1, 2, 3, 4$. We disregard here CP-violation effects, so matrix U is assumed to be real. In the limit of small mixing $\nu_e \approx \nu_1$, $\nu_\mu \approx \nu_2$, $\nu_\tau \approx \nu_3$, and $\nu_s \approx \nu_4$. We know, however, that the real mixing between active neutrinos is large and they cannot be taken as a dominant single mass eigenstate.

Kinetic equations for the density matrix of oscillating neutrinos have the usual form [23]:

$$i\dot{\rho} = [\mathcal{H}^{(1)}, \rho] - i\{\mathcal{H}^{(2)}, \rho\} \quad (4)$$

where the first commutator term includes vacuum Hamiltonian and effective potential of neutrinos in medium calculated in the first order in Fermi coupling constant, G_F . The

effective potential is proportional to the deviation of neutrino refraction index from unity and is calculated in ref. [24]. The second anti-commutator term includes imaginary part of the Hamiltonian calculated in the second order in G_F ¹. This term describes breaking of coherence induced by neutrino scattering and annihilation as well as neutrino production by collisions in primeval plasma.

Written in components kinetic equations have the form:

$$i\dot{\rho}_{ss} = \sum_a \mathcal{H}_{sa}^{(1)}(\rho_{as} - \rho_{sa}) \quad (5)$$

$$i\dot{\rho}_{aa} = \sum_b \mathcal{H}_{ab}^{(1)}(\rho_{ba} - \rho_{ab}) + \mathcal{H}_{as}^{(1)}(\rho_{sa} - \rho_{as}) - iI_{coll}(\rho) \quad (6)$$

$$i\dot{\rho}_{ab} = \mathcal{H}_{as}^{(1)}\rho_{sb} - \mathcal{H}_{sb}^{(1)}\rho_{as} + \sum_c \left(\mathcal{H}_{ac}^{(1)}\rho_{cb} - \mathcal{H}_{cb}^{(1)}\rho_{ac} \right) - i\gamma_{ab}\rho_{ab} \quad (7)$$

$$i\dot{\rho}_{sa} = \mathcal{H}_{ss}^{(1)}\rho_{sa} - \mathcal{H}_{sa}^{(1)}\rho_{ss} + \sum_b \left(\mathcal{H}_{sb}^{(1)}\rho_{ba} - \mathcal{H}_{ba}^{(1)}\rho_{sb} \right) - i\gamma_{as}\rho_{sa} \quad (8)$$

where a, b, c label active neutrino species. Matrix elements of the first order Hamiltonian $\mathcal{H}_{\alpha\beta}^{(1)} = \mathcal{H}_{\beta\alpha}^{(1)}$ (below we will omit the upper index 1) are given by:

$$\mathcal{H}_{\alpha\beta} = V_{\alpha\beta} + \sum_{j=1-4} (m_j^2/2E)U_{\alpha j}U_{\beta j} \quad (9)$$

where E is the neutrino energy and α and β run over all neutrino flavors, active and sterile. The effective potential in the medium, $V_{\alpha\beta}$, vanishes if any α or β are equal to s . For active neutrinos diagonal components of the potential are given by [24]:

$$V_{aa} = \pm C_1 \eta^{(a)} G_F T^3 - C_2^a \frac{G_F^2 T^4 E}{\alpha} \quad (10)$$

where T is the plasma temperature, G_F is the Fermi coupling constant, $\alpha = 1/137$ is the fine structure constant, and the signs “ \pm ” refer to neutrinos and anti-neutrinos respectively. The first term arises due to charge asymmetry in the primeval plasma, while the second one comes from non-locality of weak interactions associated with the exchange of W or Z bosons. According to ref. [24] the coefficients C_j are: $C_1 \approx 0.95$, $C_2^e \approx 0.61$ and $C_2^{\mu,\tau} \approx 0.17$ (for $T < m_\mu$). These values are true in the limit of thermal equilibrium, otherwise these coefficients are some integrals from the distribution functions over momenta. The charge asymmetry of plasma is described by the coefficients $\eta^{(a)}$ which are equal to

$$\eta^{(e)} = 2\eta_{\nu_e} + \eta_{\nu_\mu} + \eta_{\nu_\tau} + \eta_e - \eta_n/2 \text{ (for } \nu_e \text{)}, \quad (11)$$

$$\eta^{(\mu)} = 2\eta_{\nu_\mu} + \eta_{\nu_e} + \eta_{\nu_\tau} - \eta_n/2 \text{ (for } \nu_\mu \text{)}, \quad (12)$$

and $\eta^{(\tau)}$ for ν_τ is obtained from eq. (12) by the interchange $\mu \leftrightarrow \tau$. The individual charge asymmetries, η_X , are defined as the ratio of the difference between particle-antiparticle number densities to the number density of photons with the account of the 11/4-factor emerging from e^+e^- -annihilation:

$$\eta_X = (N_X - N_{\bar{X}})/N_\gamma \quad (13)$$

If $\nu\nu$ -interactions are essential then off-diagonal components V_{ab} are non-vanishing [25] (see also recent discussion in refs. [26]-[28]). These components are proportional to the

¹Here and in the following we will use a natural system of unit in which $\hbar = c = 1$.

integrals over neutrino momenta from off-diagonal components of the density matrix. In the case under consideration these non-diagonal components of the effective potential are sub-dominant (see sec. 5) and will be neglected.

The coherence breaking terms in off-diagonal components of the density matrix are given by $\gamma_{\alpha\beta} = (\gamma_\alpha + \gamma_\beta)/2$, where $\gamma_s = 0$ and γ_a is the total reaction rate, including elastic scattering and annihilation of ν_a :

$$\gamma_a = g_a \frac{180\zeta(3)}{7\pi^4} G_F^2 T^4 p. \quad (14)$$

Here p is the neutrino momentum and the coefficients g_a , according to ref. [19] are $g_{\nu_e} \simeq 4$ and $g_{\nu_\mu, \mu_\tau} \simeq 2.9$. Slightly smaller results $g_{\nu_e} \simeq 3.56$ and $g_{\nu_\mu, \mu_\tau} \simeq 2.5$ were obtained in ref. [29] due to account of Fermi statistics.

The coherence breaking terms in kinetic equations for diagonal components of density matrix, ρ_{aa} , are given by

$$\begin{aligned} I_{coll} = & \frac{1}{2E_1} \sum \int d\tau(l_2, \nu_3, l_4) |A_{el}|^2 [\rho_{aa}(p_1) f_l(p_2) - \rho_{aa}(p_3) f_l(p_4)] - \\ & \frac{1}{2E_1} \sum \int d\tau(l_2, \nu_3, l_4) |A_{ann}| [\rho_{aa}(p_1) \bar{\rho}_{aa}(p_2) - f_l(p_3) f_{\bar{l}}(p_4)] \end{aligned} \quad (15)$$

where $A_{el, ann}$ are the amplitudes of the corresponding reactions and the sum is taken over all possible channels of elastic scattering (first term) and annihilation (second term). The phase space element is given by:

$$d\tau(l_2, \nu_3, l_4) = (2\pi)^4 \delta^4(p_1 + p_2 - p_3 - p_4) \frac{d^3 p_2}{2E_2 (2\pi)^3} \frac{d^3 p_3}{2E_3 (2\pi)^3} \frac{d^3 p_4}{2E_4 (2\pi)^3} \quad (16)$$

It is noteworthy that in the absence of annihilation $\bar{\nu}_a \nu_a \leftrightarrow e^+ e^-$ the total number density of all neutrinos is conserved in comoving volume:

$$a^3(t) \int \frac{d^3 p}{(2\pi)^3} \left(\rho_{ss} + \sum_a \rho_{aa} \right) = const \quad (17)$$

where $a(t)$ is the cosmological scale factor. At the temperatures below freezing of the reactions $\nu_a \bar{\nu}_a \leftrightarrow e^+ e^-$ ($T_{\nu_e}^f \approx 3.2$ MeV and $T_{\nu_\mu, \nu_\tau}^f \approx 5.3$ MeV [20, 30], see also sec. 3.2) sterile neutrino states are produced at the expense of active ones and the effective number of additional neutrino species does not change. However the effect of the oscillations on BBN would be noticeable even in this case because of the deficit of ν_e induced either by direct mixing $\nu_e - \nu_s$ or by mixing of $\nu_{\mu, \tau} - \nu_s$ and fast redistribution of active neutrino species due to large mixing between them.

Concluding this section, we introduce convenient variables in terms of which we will solve kinetic equations:

$$x = ma(t) = m/T, \quad y = Ea(t) = E/T \quad (18)$$

where m is an arbitrary normalization mass which for convenience is taken as 1 MeV and $a(t)$ is the cosmological scale factor. We assume that the temperature evolves as $T = 1/a(t)$. Though it is not always true, the precision of this assumption is sufficiently good for our purposes. In terms of these variables the l.h.s. of kinetic equations in Friedman-Robertson-Walker background can be rewritten as

$$\dot{f} = (\partial_t - Hp\partial_p) f = Hx\partial_x f \quad (19)$$

where $H = \dot{a}/a$ is the Hubble parameter.

Expressed through x and y , essential quantities take the following forms:

$$H = h/x^2, \text{ with } h = 4.46 \cdot 10^{-22} (g_*/10.75)^{1/2} \quad (20)$$

where g_* is the number of species in the primeval plasma; $g_* = 10.75$ for $T < m_\mu$; we have neglected here presumably small (< 1) contribution from ν_s . The energy difference of neutrinos is given by

$$\delta E \equiv \frac{\delta m^2}{2E} = 5 \cdot 10^{-13} \left(\delta m^2 / \text{eV}^2 \right) (x/y) \equiv d_m(x/y) \quad (21)$$

Below we will always measure neutrino mass difference in eV^2 if not stated otherwise. The “non-local” contribution to neutrino potential in matter (the second term in eq. (10)) is equal to

$$V_{nl}^{(a)} = C_v^{(a)}(y/x^5) \quad (22)$$

where $C_v^{(e)} = 1.137 \cdot 10^{-20}$ and $C_v^{(\mu)} = C_v^{(\tau)} = 0.317 \cdot 10^{-20}$. Contribution to the potential from charge asymmetry of primeval plasma is always sub-dominant if η has “normal value $10^{-9} - 10^{-10}$ ”. The case of non-negligible charge asymmetry is considered in sec. 7. The coherence breaking terms determined by γ have the same dependence on x and y as $V_{nl}^{(a)}$ but with much smaller coefficient. Still they should be retained because only they contribute into imaginary parts of the density matrix and create exponential damping. They are given by:

$$\gamma_{ab} = \epsilon_{ab}(y/x^5) \quad (23)$$

where $\epsilon_{ee} = 1.5 \cdot 10^{-22}$ and $\epsilon_{\mu\mu} = \epsilon_{\tau\tau} = 1.1 \cdot 10^{-22}$.

3 Preliminary considerations

In this section we introduce some approximations and discuss some features of cosmological evolution of neutrinos which can be helpful for determination of numerical and analytical solutions of kinetic equations and for description of the effects of neutrino oscillations on BBN.

3.1 Stationary point approximation

Brute force numerical solution of integro-differential kinetic equations (5-8) is rather difficult and for large mass differences suffers from numerical instabilities, especially in the resonance case. On the other hand, for small mass differences numerical calculations can be rather accurately performed.

In order to avoid numerical problems, in this work we have used an approximate but rather accurate method discussed in ref. [30, 31]. If damping terms, given by $\gamma_{\alpha\beta}\rho_{\alpha\beta}$, are sufficiently large, differential equations for off-diagonal components of density matrix can be formally solved in the stationary point approximation. It simply means that r.h.s. of these equations is assumed to be equal to zero and they reduce to linear algebraic equations (see eqs. (33,34) below). Such approximation works well when reaction rates are large, much higher than expansion rate. The latter is true for sufficiently large mass differences of oscillating neutrinos. It can be shown [14] (and it follows from the calculations presented

below) that in non-resonance case, the maximum production rate of sterile neutrinos takes place at the temperature

$$T_{prod}^{\nu_s} = (10.8, 13.4) (3/y)^{1/3} (\cos 2\theta)^{1/6} (\delta m^2/\text{eV}^2)^{1/6} \text{ MeV} \quad (24)$$

The first number above is for mixing of ν_s with ν_e , while the second one is for mixing with ν_μ or ν_τ . Thus for $\cos 2\theta \delta m^2 > 10^{-6} \text{ eV}^2$ the production of sterile neutrinos is efficient when $\Gamma \gg H$ and stationary point approximation is sufficiently accurate.

In this approximation one can express algebraically all off-diagonal components of (4×4) density matrix of oscillating neutrinos through 4 diagonal components, ρ_{aa} ($a = e, \mu, \tau$) and ρ_{ss} . This is true if the off-diagonal components of effective potential of active neutrinos can be neglected (see sec. 5). Found in this way expressions for off-diagonal components of the density matrix can be inserted into eqs. (5-6) and we obtain a closed system of integro-differential equations for the diagonal components. The latter can be easily solved numerically as is done in the following sections.

We remark that, while we have used quasi-stationary approximation for massive calculations, we have checked the validity of this approximation by solving numerically the whole system of equations (i.e. without using the stationary point approximation) for several representative values of the parameters. This more exact approach takes much more computer time but we have not encountered any problem otherwise. These more accurate results are always in a very good agreement with those obtained with the approximate code.

3.2 Kinetic equilibrium approximation

Solution of kinetic equations is conceptually simpler in the case of a large mass difference between neutrinos. In this case production of ν_s predominantly takes place at the temperatures (24) which are much larger than the neutrino decoupling temperature (situation may be different for the resonance case, see below sec. 4). Thus at least for non-resonance transition the distributions of active neutrinos should be close to the equilibrium one.

We will estimate neutrino decoupling temperatures in the Boltzmann approximation, i.e. we will assume $f_{eq} = \exp(-E/T) = \exp(-y)$. Under this assumption, if we take into account only direct reaction terms in the collision integral, the evolution of the distribution of non-oscillating neutrinos is governed by the equation:

$$Hx \frac{\partial f_\nu}{f_\nu \partial x} = -\frac{G_F^2 D y}{3\pi^3 x^5} \quad (25)$$

where the coefficient D is equal to $80(1 + g_L^2 + g_R^2)$ if all reactions in which neutrino can participate are taken into account. Here $g_L = \pm 1/2 + \sin^2 \theta_W$ and $g_R = \sin^2 \theta_W$, plus or minus in g_L stand respectively for ν_e or $\nu_{\mu, \tau}$. The weak mixing angle θ_W is experimentally determined as $\sin^2 \theta_W = 0.23$. Correspondingly the decoupling temperatures with respect to the total reaction rate are $T_{\nu_e} = 1.34 \text{ MeV}$ and $T_{\nu_{\mu, \tau}} = 1.5 \text{ MeV}$. For this and the following simplified estimates the thermally average value $\langle y \rangle = 3$ was taken.

On the other hand, neutrino re-population, as one can see from eq. (6), is determined by the much weaker (inverse) annihilation rate. As a consequence, in some range of temperatures, active neutrinos may be in kinetic but not in chemical equilibrium. In Boltzmann approximation this corresponds to:

$$\rho_{aa}(x, y) = n_a(x) \exp(-y) \quad a = e, \mu, \tau \quad (26)$$

In particular, if annihilation of active neutrinos into e^+e^- -pairs is switched-off the total number density of active plus sterile neutrinos is conserved. The rate of annihilation $\bar{\nu}\nu \leftrightarrow$

e^+e^- is given by eq. (25) with $D = 16(g_L^2 + g_R^2)$ and the decoupling temperatures would be $T_{\nu_e}^d = 3.2$ MeV and $T_{\nu_\mu, \nu_\tau}^d = 5.34$ MeV. Below these temperatures the total number density of all four neutrino flavors in comoving volume could not change. So extra neutrino species are not created, though redistribution between ν_a and ν_s is possible.

In order to keep the computation time reasonably low, we assumed that, in the considered parameter range, the active neutrino distribution functions are conveniently described by eq. (26). For ρ_{ss} we did not make any simplifying assumption and took it as an arbitrary function of time and energy. Let us remark that, while we used kinetic equilibrium approximation for massive calculations, we have also solved numerically, for several values of the parameters, the whole system of integro-differential equations (i.e. assuming neither kinetic equilibrium nor stationary point approximations). The results obtained are always in a very good agreement with those obtained by using the approximate code.

3.3 Effects on BBN

One should also keep in mind that BBN is especially sensitive to the number density of electronic neutrinos because the latter directly participate in reactions of neutron-proton transformation. A depletion of ν_e and equally $\bar{\nu}_e$ number densities ² through oscillations would give rise to a larger neutron freezing temperature and to a larger abundances of primordial deuterium and helium-4, thus enhancing the effect of the ν_s contribution into the energy density of the universe. The described effect can be simply taken into account, if we assume that electron neutrinos are in kinetic equilibrium, that the Boltzmann statistics is valid, and neglect the electron mass. In this assumption, the neutron to proton interconversion rate Γ_{np} is proportional to $\Gamma_{np} = (1 + n_e)/2$. This means that the neutron freezing temperature scales as:

$$T_f \propto \left[\frac{g_*^{1/2}}{(1 + n_e)/2} \right]^{1/3} \quad (27)$$

where $g_* = 10.75 + (7/4)\Delta N_\nu$, and thus the global effect on BBN can be described as a variation of the effective number of neutrino species:

$$\Delta N_\nu^{\text{BBN}} = \frac{4}{7} \left[\frac{10.75 + (7/4)\Delta N_\nu}{((1 + n_e)/2)^2} - 10.75 \right] \quad (28)$$

If we consider possible deviations from kinetic equilibrium, the same formulas apply but we have to replace n_e by:

$$\langle n_e \rangle = \frac{\int_0^\infty dy y^2 (y + \Delta m/T)^2 \rho_{ee}(x, y)}{\int_0^\infty dy y^2 (y + \Delta m/T)^2 e^{-y}}, \quad (29)$$

where $\Delta m = 1.3$ MeV is the neutron-proton mass difference and T is the temperature.

If only one active and one sterile neutrinos were mixed, while mixing among the active neutrinos was absent the described effect would lead to a stronger restriction on the mixing angle in low δm^2 region in the case of $(\nu_e - \nu_s)$ -mixing. In the case of ν_μ or ν_τ mixing with ν_s the effect is less pronounced because depletion of ν_e is now a two step process. First, the number density of ν_μ or ν_τ decreases due to transition into ν_s and after that some re-population of $\nu_{\mu, \tau}$ by $\bar{\nu}_e \nu_e \rightarrow \bar{\nu}_{\mu, \tau} \nu_{\mu, \tau}$ occurs at the expense of the number density of ν_e .

²In the resonance case ν_e and $\bar{\nu}_e$ can be depleted by a different amount and a noticeable charge asymmetry between active neutrinos can be created. This is discussed in sec. 7

This process however is not very efficient because to be noticeable it should take place after decoupling of neutrinos from e^+e^- plasma but practically simultaneously neutrinos decouple from themselves. However if the active neutrino species are mixed then the depopulation of ν_e would be much stronger as we see in what follows.

4 Mixed one active and one sterile neutrinos

As a first step let us consider the case when mutual mixing of active neutrinos is absent and only one active neutrino is mixed with the sterile neutrino. Previous BBN constraints on sterile neutrino admixture have been derived under this assumption. We present below the results of our numerical calculations together with some useful analytic estimates both for the non-resonance and resonance cases.

4.1 Non-resonance case

The density matrix of the *oscillating* neutrinos is 2×2 . It contains only four real functions: ρ_{aa} , ρ_{ss} , and $\rho_{as} = \rho_{sa}^* = R + iI$, which have to be determined from the solution of kinetic equations:

$$Hx \partial_x \rho_{aa} = i\mathcal{H}_{as}(\rho_{as} - \rho_{sa}) - I_{coll}(q) \quad (30)$$

$$Hx \partial_x \rho_{ss} = -i\mathcal{H}_{as}(\rho_{as} - \rho_{sa}) \quad (31)$$

$$Hx \partial_x \rho_{as} = -i[(\mathcal{H}_{aa} - \mathcal{H}_{ss}) - i\gamma_{as}] \rho_{as} + i\mathcal{H}_{as}(\rho_{aa} - \rho_{ss}) \quad (32)$$

The formal solution of equation (32) is:

$$\rho_{as} = i \int_0^x dx_1 \frac{\mathcal{H}_{as}(\rho_{aa} - \rho_{ss})_1}{(Hx)_1} \exp \left[-i \int_{x_1}^x dx_2 \frac{(\mathcal{H}_{aa} - \mathcal{H}_{ss} - i\gamma_{as})_2}{(Hx)_2} \right] \quad (33)$$

where the indices sub-1 and sub-2 indicate that the corresponding expressions are taken at x_1 or x_2 . If γ_{as} is large (more precisely we require $\gamma_{as}/H \gg 1$) then the integrals "sit" on the upper limit $x_1 = x_2 = x$ and in this way the stationary point result is obtained:

$$\rho_{as} = \frac{\mathcal{H}_{as}}{(\mathcal{H}_{aa} - \mathcal{H}_{ss}) - i\gamma_{as}} (\rho_{aa} - \rho_{ss}) . \quad (34)$$

This result is valid both for resonance and non-resonance cases if the mass difference is sufficiently large, but the limits of applicability are somewhat different. As is mentioned above, for non-resonance case the temperature of ν_s production (24) should be higher than the decoupling temperature with respect to total reaction rate. This condition is satisfied for ν_e if $\delta m^2 > 3.7 \cdot 10^{-6} \text{ eV}^2$ and for $\nu_{\mu,\tau}$ if $\delta m^2 > 2 \cdot 10^{-6} \text{ eV}^2$. The resonance case is considered in the following section.

Substituting the result (34) into eq. (31) we find:

$$Hx \partial_x \rho_{ss} = 2 \frac{\gamma_{as} \mathcal{H}_{as}^2}{(\mathcal{H}_{aa} - \mathcal{H}_{ss})^2 + \gamma_{as}^2} (\rho_{aa} - \rho_{ss}) \quad (35)$$

which, in terms of the mass difference, δm^2 , and of the vacuum mixing angle ³, θ , can be rewritten as:

$$Hx \partial_x \rho_{ss} = \frac{\gamma_a}{4} (\rho_{aa} - \rho_{ss}) \frac{\sin^2 2\theta}{(\cos 2\theta - V_{aa}/\delta E)^2 + \gamma_a^2/4\delta E^2} \quad (36)$$

³In our notations, δm^2 is positive if sterile neutrino is heavier than active neutrino, in the limit $\theta \rightarrow 0$. Non resonance cases correspond to positive δm^2 .

From this expression (neglecting the γ^2 -term in the denominator) follows that the rate of production of sterile neutrinos in the primeval plasma is equal to:

$$\gamma_s = \frac{1}{4} \gamma_a \tan^2 2\theta_m \quad (37)$$

where θ_m is the effective mixing angle in matter given by the last factor in eq. (36). This result is twice smaller than simple estimates presented in earlier papers [14]-[18].

In non-resonance case, when $\cos 2\theta \delta E - V_{aa} \neq 0$ (i.e. $\delta m^2 > 0$) and one may neglect the γ^2 -term in the denominator, the number of additional neutrino species ΔN_ν at BBN can be analytically calculated from eq. (36) in the limit of $\rho_{ss} \ll \rho_{aa}$ and $\rho_{aa} = f_{eq}$. In this approximation we obtain:

$$(\delta m^2_{\nu_e \nu_s} / \text{eV}^2) \sin^4 2\theta^{\nu_e \nu_s} = 3.16 \cdot 10^{-5} (\Delta N_\nu)^2 \quad (38)$$

$$(\delta m^2_{\nu_\mu \nu_s} / \text{eV}^2) \sin^4 2\theta^{\nu_\mu \nu_s} = 1.74 \cdot 10^{-5} (\Delta N_\nu)^2 \quad (39)$$

If ΔN_ν is not small, then ρ_{ss} in eq. (36) should be included and a better approximation in the bounds above would be given by the factor $\ln^2(1 - \Delta N_\nu)$ instead of $(\Delta N_\nu)^2$.

The described results are noticeably weaker than earlier obtained analytical bounds. They well agree, instead, with our numerical calculations and with those of ref. [19]. Our numerical results are presented in figs. 1 ($\nu_\mu - \nu_s$ mixing) and 2 ($\nu_e - \nu_s$ mixing). In the first panel, we show the effects of oscillations on the energy density of ν_e . Specifically, we show the lines which correspond in the plane $(\sin^2 2\theta, \delta m^2)$ to fixed, but different, values of the energy density of electron neutrinos (normalized to the equilibrium value)⁴. In the second panel, we show the energy density of sterile neutrinos. In the third panel we show the total neutrino contribution to the energy density, each line corresponding to a certain value of the number of extra neutrino flavors ΔN_ν . If there was not an additional impact of ν_e on the neutron-proton transformations, these lines would present BBN bounds on mixing parameters. The total effect of oscillations on BBN, including the impact of ν_e on $n - p$ transformation according to eq. (28), is demonstrated in the fourth panel in terms of the effective number of neutrino species $\Delta N_\nu^{\text{BBN}}$. Finally, we show with red dotted lines the approximate analytical results described above. Numerical calculations were made by using stationary point and kinetic equilibrium (for active neutrinos) approximation. We checked by comparing with the complete calculations, that these approximations do not introduce significant errors.

As one can see, the bounds (38,39) are reasonably accurate for large mass differences since, in this case, re-population of active neutrinos is very efficient and we can always assume $\rho_{aa} = f_{eq}$. On the contrary, when δm^2 is small (say, $\delta m^2 \leq 10^{-3} \text{ eV}^2$) significant deviations are expected. In this case, sterile neutrino production takes place at low temperatures, see eq. (24), when inverse annihilation processes become slow with respect to the expansion rate of the universe. Slow re-population of active neutrinos results in a decrease of ΔN_ν , since the production of ν_s goes at the expense of diminishing the number density of ν_a .

In the case of $\nu_e - \nu_s$ mixing, the decrease in the number density of ν_e and $\bar{\nu}_e$ results in a decrease of the neutron-to-proton inter-conversion rates which leads to a higher temperature of neutron freezing and to larger neutron-to-proton ratio and, as a result, to higher abundances of D and ${}^4\text{He}$. This effect can be effectively described as an increase in $\Delta N_\nu^{\text{BBN}}$ which is much larger than the simultaneous decrease of ΔN_ν produced by the decrease of

⁴Numerical calculations have been mostly done in the assumption of kinetic equilibrium for active neutrinos, as explained in sect. 3.3. In this assumption, the energy density of ν_e (normalized to equilibrium value) is simply equal to the value of the overall normalization factor n_e defined in eq. (26).

ν_e number density. This means that, for small δm^2 , the BBN bound on $\nu_e - \nu_s$ oscillations is considerably stronger than that obtained from the simple estimate given by eq.(38).

It is important to remark that in the case of $\nu_\mu - \nu_s$ ($\nu_\tau - \nu_s$) mixing, one expects a depletion of ν_e too. The number density of ν_μ (or ν_τ) goes down due to transformation of these particles into ν_s . This opens window for $\bar{\nu}_e \nu_e \rightarrow \bar{\nu}_{\mu,\tau} \nu_{\mu,\tau}$ and to a decrease of number density of ν_e . In this case, however, the effect is considerably smaller and it has a magnitude comparable to the the decrease of ΔN_ν produced by the decrease of ν_μ (ν_τ) number density.

4.2 Resonance case. Analytic estimates

Situation in the resonance case (i.e. when $\delta m^2 < 0$) is somewhat more complicated both from the point of view of analytical and numerical calculations. We show, in this section, that simple analytical estimates can be obtained even in this case.

Let us return to kinetic equations (30,31). We assume that the collision integral $I_{coll}(q)$ has a negligible role during resonance. In other words, we assume that *during resonance* neutrinos are neither effectively created nor scattered by other particles. This approximation is justified because the characteristic "time" of collisions/annihilation, $\delta x_{coll} \sim \gamma/H$, is much longer than the inverse resonance width, $\delta x_{res} \sim \gamma/\delta E$, in the essential range of parameters. We maintain, however, the decoherence term in the equations for the non-diagonal terms of the density matrix. Under this assumptions, neutrino evolution *during resonance* is described by the equations:

$$Hx \partial_x (\rho_{aa} + \rho_{ss}) = 0 \quad (40)$$

$$Hx \partial_x (\rho_{aa} - \rho_{ss}) = 2i \mathcal{H}_{as} (\rho_{as} - \rho_{sa}) \quad (41)$$

where $\rho_{as} = \rho_{sa}^*$ and the non diagonal term ρ_{as} is given by eq.(33). We can write formally:

$$\rho_{as}(x, y) = i \exp(-F(x, y)) \int_0^x dx_1 \frac{[\mathcal{H}_{as}(\rho_{aa} - \rho_{ss})]_1}{(Hx)_1} \exp(F(x_1, y)) \quad (42)$$

where the function $F(x, y)$ is defined by the condition:

$$Hx \partial_x F(x, y) = i (\mathcal{H}_{aa} - \mathcal{H}_{ss} - i\gamma_{as}) \quad (43)$$

From the above expression, we see that the function $F(x, y)$ has stationary points z_{res} in the complex plane where:

$$\mathcal{H}_{aa}(z_{res}, y) - \mathcal{H}_{ss}(z_{res}, y) - i\gamma_{as}(z_{res}, y) = 0 \quad (44)$$

We can explicitly solve this equation, obtaining:

$$(z_{res})_n = \left(\frac{y^2 (|C_v^a| + i\epsilon_{as})}{|d_m| \cos(2\theta)} \right)^{1/6} \simeq \left(\frac{y^2 |C_v^a|}{|d_m| \cos(2\theta)} \right)^{1/6} \left[1 + \frac{i}{6} \delta_a \right] \exp \left(i \frac{\pi n}{3} \right) \quad (45)$$

where $n = 0, 1, \dots, 5$, the parameters d_m , C_v^a and ϵ_{as} are defined in eqs. (21)-(23) and $\delta_a \equiv |\epsilon_{as}/C_v^a| \sim 10^{-2}$. One can see that the usual resonance condition, $\mathcal{H}_{aa}(x_{res}, y) - \mathcal{H}_{ss}(x_{res}, y) = 0$, gives the resonance point x_{res} :

$$x_{res} = \left(\frac{y^2 |C_v^a|}{|d_m| \cos(2\theta)} \right)^{1/6} \quad (46)$$

which is essentially equal to $x_{res} \simeq \text{Re}((z_{res})_0)$.

We can take the integral (42) by using the saddle point approach:

$$\begin{aligned} \rho_{as}(x, y) &= i\sqrt{2\pi} \exp[-F(x, y) + F(z_{\text{res}}, y)] \theta(x - x_{\text{res}}) \\ &\times \left[\frac{\mathcal{H}_{as}}{(Hx)} \right]_{\text{res}} \left| \frac{\partial^2 F}{\partial x^2} \right|_{\text{res}}^{-1/2} \exp\left(i\frac{\pi}{2} - i\frac{1}{2}\psi\right) (\rho_{aa} - \rho_{ss})_{\text{res}} \end{aligned} \quad (47)$$

where the index [res] indicate that the various quantities are evaluated at $z_{\text{res}} = (z_{\text{res}})_0$, and the phase ψ is given by $\psi = \arg(\partial^2 F / \partial x^2)_{\text{res}}$. We remark that the second derivative of the function $F(x, y)$ at resonance, can be expressed through the simple formula:

$$\frac{\partial^2 F(x, y)}{\partial x^2} = \frac{(\mathcal{H}_{aa}^{\text{vac}} - \mathcal{H}_{ss}^{\text{vac}})_{\text{res}}}{(Hx)_{\text{res}}} \frac{6i}{z_{\text{res}}} \quad (48)$$

where \mathcal{H}^{vac} is the vacuum hamiltonian, from which we see that $\psi \sim \pi/2$.

Equation (47) describes the approximate behavior of $\rho_{as}(x, y)$ as a function of neutrino parameters and of the difference $(\rho_{aa} - \rho_{ss})_{\text{res}}$ at the resonance. We can use this expression to integrate eqs. (40,41). We have:

$$(\rho_{aa} + \rho_{ss}) = \text{const} \quad (49)$$

$$\Delta(\rho_{aa} - \rho_{ss}) = 2i \int_0^x dx_0 \frac{(\mathcal{H}_{as})_0}{(Hx)_0} (\rho_{as} - \rho_{sa})_0 \quad (50)$$

where $\Delta(\rho_{aa} - \rho_{ss})$ is the total variation of $(\rho_{aa} - \rho_{ss})$ across resonance. If we integrate the previous equations using, one more time, the saddle point approach, we obtain:

$$\Delta(\rho_{aa} - \rho_{ss}) = -2\pi(\rho_{aa} - \rho_{ss})_{\text{res}} \left| \frac{\partial^2 F}{\partial x^2} \right|_{\text{res}}^{-1} \left[\left(\frac{(\mathcal{H}_{as})_{\text{res}}}{(Hx)_{\text{res}}} \right)^2 \exp\left(i\frac{\pi}{2} - i\psi\right) + c.c. \right] \quad (51)$$

This expression can be calculated explicitly, giving:

$$\begin{aligned} \Delta(\rho_{aa} - \rho_{ss}) &= -\frac{\pi}{6} \frac{|d_m| \sin^2(2\theta)}{h \cos(2\theta)} \text{Re} \left(\frac{z_{\text{res}}^3}{y} \right) (\rho_{aa} - \rho_{ss})_{\text{res}} \\ &= -\frac{\pi}{6} \frac{|d_m| \sin^2(2\theta)}{h \cos(2\theta)} \text{Re} \left(\frac{|C_v^a| + i\epsilon_{es}}{|d_m| \cos(2\theta)} \right)^{1/2} (\rho_{aa} - \rho_{ss})_{\text{res}} \end{aligned} \quad (52)$$

As a final result, we have thus obtained an algebraic relation between the value of the difference $(\rho_{aa} - \rho_{ss})$ at the resonance, $(\rho_{aa} - \rho_{ss})_{\text{res}}$, and its *total variation* $\Delta(\rho_{aa} - \rho_{ss})$.

If we assume that $\Delta(\rho_{aa} - \rho_{ss})$ is small, the value of $(\rho_{aa} - \rho_{ss})$ at resonance is close to its initial value, i.e. $(\rho_{aa} - \rho_{ss})_{\text{res}} \simeq (\rho_{aa})_{\text{in}}$. In this assumption, we immediately obtain from eqs. (52,49) an estimate for active (sterile) neutrino depletion (production) due to resonance. We have:

$$P_{aa} \equiv \frac{(\rho_{aa})_{\text{in}} + \Delta\rho_{aa}}{(\rho_{aa})_{\text{in}}} = 1 - K \quad (53)$$

$$P_{as} \equiv \frac{\Delta\rho_{ss}}{(\rho_{aa})_{\text{in}}} = K \quad (54)$$

where

$$K = \frac{\pi}{12} \frac{|d_m| \sin^2(2\theta)}{h \cos(2\theta)} \text{Re} \left(\frac{y^2 (|C_v^a| + i\epsilon_{es})}{|d_m| \cos(2\theta)} \right)^{1/2} \simeq A_a \left(\frac{|\delta m^2|}{eV^2} \right)^{1/2} \frac{\sin^2(2\theta)}{\cos(2\theta)^{3/2}} \quad (55)$$

The coefficient A_a is equal to $A_e = 4.4 \cdot 10^4$ for $\nu_e - \nu_s$ mixing and $A_{\mu,\tau} = 2.3 \cdot 10^4$ for $\nu_\mu - \nu_s$ or $\nu_\tau - \nu_s$ mixing. The previous equations represent our final results. A few comments are in order:

1. These simple formulas, in the range of parameters in which they are valid (i.e. small K and, thus, small mixing angles), well agree with the results obtained by describing resonance effects by Landau-Zener approach [39]. We recall that, in this scheme, the active (sterile) neutrino survival (oscillation) probability P_{aa} (P_{as}) is given by:

$$P_{aa} = P_c \quad (56)$$

$$P_{as} = 1 - P_c \quad (57)$$

where:

$$P_c = \exp(-K) \quad (58)$$

and we assumed $\sin 2\theta \ll 1$. The agreement between our simple formulas, which take into account decoherence effects, with the Landau Zener results (which do not take them into account), in the range of parameter in which our formulas are valid, makes us confident of the validity of eqs. (56,57) in the whole parameter space. In the following we will use Landau-Zener formulas to obtain simple analytic predictions for the whole range of masses and mixing angles.

2. As also noted by [19], momentum dependence disappears from eqs. (56,57) (and (53,54)). This means that resonance does not produce, as a net result ⁵, a strong spectral distortion of neutrino distributions. As a consequence, the probabilities P_{aa} and P_{as} can be taken, in first approximation, as global multiplicative factors of active and sterile neutrino distribution functions.

So far we have considered neutrino evolution through resonance. Post resonance evolution is simple if the mixing angle is sufficiently small. In this case, after resonance, sterile neutrinos are not produced. We have then:

$$\frac{\rho_{ss}(x, y)}{\rho_{aa}(x, y)_{in}} = P_{as} = \text{const} \quad x > x_{res} \quad (59)$$

On the other hand, active neutrino distribution function evolves due annihilation and/or scattering, as described by the collision integral $I_{coll}(q)$. A simple description can be obtained if active neutrinos are approximately in kinetic equilibrium. Under this assumption, the time evolution of the normalization factor n_a is described by the equation:

$$\frac{dn_a(x)}{dx} = -\langle \gamma_{ann} \rangle [n_a(x)^2 - 1] \quad (60)$$

where the symbol $\langle \dots \rangle$ indicates averaging over the Maxwell-Boltzmann distribution and γ_{ann} is the total $\nu_a \bar{\nu}_a$ annihilation rate. If we assume that the deviation from chemical equilibrium produced by resonance is generated abruptly at the time \bar{x}_{res} when neutrinos

⁵We remark that neutrinos with different momenta go through resonance at different times, see eq. (46). This means that, while we do not expect strong distortions at the end of the process (i.e. after *all* relevant momenta have passed through resonance), a strong distortions can be generated at a given time as a result of the fact that *only some* momenta, at that time, have reached resonance.

with momentum $y = 3$ (which we take representative of the whole ensemble) goes through resonance, the previous equation can be solved explicitly giving the result:

$$n_a(x) = \frac{1 + A}{1 - A} \quad (61)$$

where

$$A = \frac{P_{aa} - 1}{P_{aa} + 1} \exp \left[-\frac{2}{3} \langle \gamma_{\text{ann}} \rangle \left(\frac{1}{x_{\text{res}}^3} - \frac{1}{x_{\text{BBN}}^3} \right) \right] \quad (62)$$

and x_{BBN}^3 is the "time" at which BBN takes place.

In figs. 3 and 4 we compare the analytical estimates with the numerical calculations. Specifically, in fig. 3 we compare, in the case of $\nu_e - \nu_s$ mixing, the prediction of eqs. (57,59) (red dotted lines) with the energy density of sterile neutrinos obtained from numerical calculations (solid lines) as functions of the mixing angle $\sin^2 2\theta$, for selected values of the mass difference δm^2 . One can see that eqs. (57,59) correctly describe the dependence of sterile neutrino production on the oscillation parameters over a wide range of masses and mixing angles. In particular, the analytical calculations are very accurate at small mixings, while they tend to overestimate sterile neutrino production at large angles. We remark that numerical results shown in fig. 3 have been obtained with the complete code (i.e. without using stationary point and kinetic equilibrium approximations) in order to be sure not to introduce the errors of approximation into the calculation. In fig. 4 we compare the analytical results (dotted lines) for n_e with the energy density of ν_e obtained from numerical calculations (solid lines). Blue dotted lines are obtained from eqs. (57) and do not take into account the post-resonance evolution of ν_e . Red dotted lines include post resonance evolution according to eq. (61). As one can see, analytic results give a correct qualitative understanding of n_e dependence on oscillation parameters.

4.3 Resonance case. Numerical calculations

Stationary point approximation (34) is also valid in the resonance case but the region of validity is found in a different way because the effective production temperature is determined by the resonance condition and not by eq. (24).

In order to discuss the validity of the stationary point approximation, we have to go back to eq. (33). The stationary point approximation follows from the expansion:

$$\begin{aligned} i \int_{x_1}^x dx_2 \frac{(\mathcal{H}_{aa} - \mathcal{H}_{ss} - i\gamma_{as})_2}{(Hx)_2} &\simeq \\ &\simeq i \frac{(\mathcal{H}_{aa} - \mathcal{H}_{ss} - i\gamma_{as})_1}{(Hx)_1} (x - x_1) + \frac{i}{2} \frac{\partial [(\mathcal{H}_{aa} - \mathcal{H}_{ss} - i\gamma_{as})/Hx]_1}{\partial x} (x - x_1)^2 \end{aligned} \quad (63)$$

of the exponent in eq. (33). Due to the fact that $\gamma_{as}/H \gg 1$, only a small region $\delta x = (x - x_1)/x_1 \simeq H/\gamma_{as}$ is important. Thus the expansion can be truncated to first order and the stationary point approximation can be easily obtained:

$$\rho_{as} = \frac{\mathcal{H}_{as}}{(\mathcal{H}_{aa} - \mathcal{H}_{ss}) - i\gamma_{as}} (\rho_{aa} - \rho_{ss}) \quad (64)$$

In resonance case the situation is more complicated. Far from the resonance, the above discussion applies without any modification. At the resonance point, instead, the factor

$(\mathcal{H}_{aa} - \mathcal{H}_{ss})$ vanishes, with the consequence that higher order terms in the expansion may become important. This does not happen when:

$$\left(\frac{x}{H}\right)_{\text{res}} \left[\frac{\partial(\mathcal{H}_{aa} - \mathcal{H}_{ss})}{\partial x} \right]_{\text{res}} \frac{\delta x^2}{2} \ll \left(\frac{\gamma_{as}}{H}\right)_{\text{res}} \delta x \quad (65)$$

where $\delta x = (H/\gamma_{as})_{\text{res}}$. In this case, which corresponds $\delta m^2 > 10^{-1} \text{ eV}^2$ for $\nu_e - \nu_s$ mixing and $\delta m^2 > 10^{-3} \text{ eV}^2$ for $\nu_\mu - \nu_s$ mixing, the first order term in the expansion is anyhow dominant and eq. (64) continues to be valid.

For smaller masses, eq. (64) is not strictly true. Specifically, this equation overestimates ρ_{as} at resonance. However, this does not introduce significant errors for the evolution of the diagonal components, since at the same time, resonance width is underestimated by a compensating amount. The most direct way to understand this is to consider the equations describing the evolution of the diagonal components which are obtained within the stationary point approximation:

$$Hx \partial_x(\rho_{aa} - \rho_{ss}) = -4 \frac{\gamma_{as} \mathcal{H}_{as}^2}{(\mathcal{H}_{aa} - \mathcal{H}_{ss})^2 + \gamma_{as}^2} (\rho_{aa} - \rho_{ss}) - I_{\text{coll}}(\rho) \quad (66)$$

Close to resonance, we can neglect the collision integral and expand the r.h.s obtaining:

$$\partial_x(\rho_{aa} - \rho_{ss}) = -4 \frac{(\gamma_{as}/Hx)_{\text{res}} (\mathcal{H}_{as}/Hx)_{\text{res}}^2}{B(x - x_{\text{res}})^2 + (\gamma_{as}/Hx)_{\text{res}}^2} (\rho_{aa} - \rho_{ss}) \quad (67)$$

where

$$B \equiv \left[\frac{\partial(\mathcal{H}_{aa} - \mathcal{H}_{ss})/Hx}{\partial x} \right]_{\text{res}} \simeq -i \left[\frac{\partial^2 F(x, y)}{\partial x^2} \right]_{\text{res}}. \quad (68)$$

The index [res] indicates that the various quantities are evaluated at the resonance point and the function $F(x, y)$ is defined in the previous section by eq. (43). If we define $\xi \equiv B(\gamma_{as}/Hx)^{-1}(x - x_{\text{res}})$, eq. (67) becomes

$$\partial_\xi(\rho_{aa} - \rho_{ss}) = -4 \frac{(\mathcal{H}_{as}/Hx)_{\text{res}}^2}{B} \frac{1}{\xi^2 + 1} (\rho_{aa} - \rho_{ss}) \quad (69)$$

One should note that the factor γ_{as} has disappeared from our formulas. We could expect then that eq. (66), derived under assumption of large γ_{as} , is valid even in the limit of small γ_{as} . We can confirm this by integrating eq. (66) assuming a slowly variation of $\rho_{aa} - \rho_{ss}$. We obtain:

$$\Delta(\rho_{aa} - \rho_{ss}) \simeq -4\pi (\mathcal{H}_{as}/Hx)_{\text{res}}^2 \left| \frac{\partial^2 F}{\partial x^2} \right|_{\text{res}}^{-1} (\rho_{aa} - \rho_{ss})_{\text{res}} \quad (70)$$

This result coincides with the expected behavior, eq. (51), and confirm the validity of the stationary point approximation in the resonance case even for small mass differences.

In fig. 5 ($\nu_\mu - \nu_s$ mixing) and in fig. 6 ($\nu_e - \nu_s$ mixing) we show our numerical results for the resonance case in the plane $(\sin^2 2\theta, \delta m^2)$. Let us remark that, besides the previous discussion, we also have checked numerically the displayed results, by comparing them, for several values of the parameters, with the results of complete numerical integration of kinetic equations. Similarly to fig. 1 and fig. 2, the first panel shows the effect of oscillations on ν_e energy density, the second panel shows the energy density of sterile neutrinos, the

third panel describes the total neutrino contribution to the energy density and, finally, the fourth panel shows the total effects of oscillations on BBN.

Our constraints on sterile neutrino admixture in the resonant case are stronger than previous results of [19], which were obtained in the context of single momentum approximation. We are not able to understand the source of the observed difference. We are however confident in the results of our numerical calculations, especially in the small mixing angles region, where, as shown in the previous section, they can be analytically understood with good accuracy.

In fig. 5 and 6 we show with red dotted lines the prediction obtained from eq. (57), which correctly reproduce (at small mixing) the numerical results. In Fig. 6 we also show the prediction which can be obtained by using eqs. (56) and (61) which give a qualitative understanding of the behavior observed for $\Delta N_\nu^{\text{BBN}}$.

5 Mixed two active and one sterile neutrinos

In the case that only two active neutrinos (say, ν_e and ν_μ) are mixed between themselves and one sterile neutrino, all algebraic manipulations are relatively easy and the resulting equations have a simple form and can be explicitly written down below. We will consider large mass differences, so for the off-diagonal elements of the density matrix the stationary point approximation may be used.

Using eq. (7) we can eliminate the $e\mu$ -off-diagonal component of the neutrino density matrix:

$$\rho_{e\mu} = \frac{\mathcal{H}_{e\mu}(\rho_{\mu\mu} - \rho_{ee}) + \mathcal{H}_{es}\rho_{s\mu} - \mathcal{H}_{\mu s}\rho_{es}}{\mathcal{H}_{\mu\mu} - \mathcal{H}_{ee} + i\gamma_{\mu\mu}} \quad (71)$$

Substituting this expression into eqs. (8) and their complex conjugate we obtain a closed system of equations for four off-diagonal component ρ_{se} , $\rho_{s\mu}$, and their complex conjugate ρ_{es} and $\rho_{\mu s}$. They can be explicitly solved in terms of $\rho_{\mu\mu}$, ρ_{ee} , and ρ_{ss} . For example,

$$\rho_{se} = (AC^* - BC) / Det \quad (72)$$

where $Det = |A|^2 - |B|^2$ is the determinant of the linear system of 4 algebraic equations for ρ_{sa} and ρ_{as} and

$$A = Z_{es}^* + \frac{\mathcal{H}_{\mu s}^2}{Z_{\mu e}} - \frac{\mathcal{H}_{e\mu}^2 Z_{\mu e}^*}{Z_{\mu s}^* Z_{\mu e}^* - \mathcal{H}_{es}^2} + \frac{(\mathcal{H}_{\mu s} \mathcal{H}_{es})^2}{Z_{\mu e} (Z_{\mu s} Z_{\mu e} - \mathcal{H}_{es}^2)} \quad (73)$$

$$B = 2 \text{Im} \left[\frac{\mathcal{H}_{\mu s} \mathcal{H}_{es} \mathcal{H}_{e\mu}}{Z_{\mu s} Z_{\mu e} - \mathcal{H}_{es}^2} \right] \quad (74)$$

$$C = S_e - \frac{\mathcal{H}_{e\mu} Z_{\mu e}^*}{Z_{\mu s}^* Z_{\mu e}^* - \mathcal{H}_{es}^2} S_\mu + \frac{\mathcal{H}_{\mu s} \mathcal{H}_{es}}{Z_{\mu s} Z_{\mu e} - \mathcal{H}_{es}^2} S_\mu^* \quad (75)$$

$$Z_{\alpha\beta} = \mathcal{H}_{\alpha\alpha}^{(1)} - \mathcal{H}_{\beta\beta}^{(1)} + i\gamma_{\alpha\beta} \quad (76)$$

$$S_e = \frac{\mathcal{H}_{e\mu} \mathcal{H}_{\mu s}}{Z_{\mu e}} (\rho_{\mu\mu} - \rho_{ee}) + \mathcal{H}_{es} (\rho_{ee} - \rho_{ss}) \quad (77)$$

S_μ and $\rho_{s\mu}$ can be obtained from eqs. (71)-(77) by the interchange of e and μ .

Analytical expressions are particularly simple in the case of weak mixing with ν_s and for sufficiently large mass differences, such that refilling of active states is fast and their

number densities approach equilibrium values, $\rho_{ee} = \rho_{\mu\mu} = f_{eq}$. The analytical limits (38) and (39) are obtained under similar assumptions. In this case the differential equation that governs evolution of ρ_{ss} takes the form:

$$\partial_x \rho_{ss} = 2(f_{eq} - \rho_{ss}) \frac{\gamma_{es} (\mathcal{H}_{es} \mathcal{H}_{\mu\mu} - \mathcal{H}_{e\mu} \mathcal{H}_{\mu s})^2 + \gamma_{\mu s} (\mathcal{H}_{\mu s} \mathcal{H}_{ee} - \mathcal{H}_{e\mu} \mathcal{H}_{es})^2}{Hx (\mathcal{H}_{ee} \mathcal{H}_{\mu\mu} - \mathcal{H}_{e\mu}^2)^2} \quad (78)$$

This result is valid in no-resonance case when $\mathcal{H}_{ee} \mathcal{H}_{\mu\mu} - \mathcal{H}_{e\mu}^2 \neq 0$. If MSW-resonance exists then one should take into account imaginary parts proportional to coherence breaking terms γ . In numerical calculations such terms have been included.

Simple expression (78) has been derived under assumption of weak mixing between active and sterile neutrinos. Relaxing this approximation we find that resonance condition is:

$$\Delta_{\mu e} \Delta_{es} \Delta_{s\mu} - \mathcal{H}_{\mu s}^2 \Delta_{\mu s} - \mathcal{H}_{es}^2 \Delta_{se} - \mathcal{H}_{e\mu}^2 \Delta_{e\mu} = 0 \quad (79)$$

where $\Delta_{\alpha\beta} = \mathcal{H}_{\alpha\alpha} - \mathcal{H}_{\beta\beta}$.

Eq. (78) justifies neglecting of non-diagonal terms in the effective potential. Indeed these non-diagonal terms are proportional to the non-diagonal components of the active-active part of neutrino density matrix. As we see from eq. (78) they should be compared to the diagonal ones. In the situation close to thermal equilibrium $\rho_{ab} = 0$ if $a \neq b$, while $\rho_{aa} = f_{eq} \sim 1$.

6 Realistic case of three active and one sterile neutrinos

Recent data from SNO [1], KamLAND [2], and earlier data on solar [3] and atmospheric [4] neutrinos have provided strong indications in favor of neutrino oscillations. It is practically established now that all active neutrinos are mixed with parameters given by the Large Mixing Angle (LMA) solution to solar neutrino problem [11], see eq. (1) and by atmospheric neutrino data [4], eq. (2). Existence of fast transitions between ν_e , ν_μ , and ν_τ may change BBN bound on mixing with sterile neutrinos especially for small values of mass difference. This means that one has to take into account mutual active neutrino mixing in the discussion of BBN bounds. Clearly the situation become much more complicated both conceptually and numerically. In the following, to keep the discussion as simple as possible, we will make the assumption that active-sterile neutrino mixing is small.

In the case of 4 mixed neutrinos the algebra becomes significantly more complicated. This is why we will not present explicit expressions for off-diagonal components of density matrix through the diagonal ones. All this work has been done by computer and the results have been inserted into differential equations for diagonal components. The latter have been solved numerically. To check the accuracy of the procedure we solved numerically the complete system of kinetic equations (5)-(8) for certain fixed values of the parameters without any simplification and found that agreement with the approximate numerical results is very good. We did not do that for all interesting values of the parameter because it would take too much computer time, especially in the resonance case.

It is clear that, depending on masses and mixing, one can expect in general case one or more resonances among active and sterile neutrinos. If ν_4 is the heaviest mass eigenstate there may only be resonances in the transformations among active neutrinos (they are quite efficient anyhow because of the strong mixing). As ν_4 is becoming lighter and lighter, there appear first one resonance in ν_a - ν_s transformation, then two and ultimately three

resonances. The resonance condition is given by the vanishing of the determinant of the 6×6 -matrix:

$$D_6 = \det \begin{vmatrix} \Delta_{e\mu} & -\mathcal{H}_{\mu\tau} & \mathcal{H}_{e\tau} & \mathcal{H}_{es} & -\mathcal{H}_{\mu s} & 0 \\ -\mathcal{H}_{\mu\tau} & \Delta_{e\tau} & \mathcal{H}_{e\mu} & 0 & -\mathcal{H}_{\tau s} & \mathcal{H}_{es} \\ -\mathcal{H}_{e\tau} & \mathcal{H}_{e\mu} & \Delta_{\mu\tau} & -\mathcal{H}_{\tau s} & 0 & \mathcal{H}_{\mu s} \\ -\mathcal{H}_{es} & 0 & -\mathcal{H}_{\tau s} & \Delta_{\mu s} & \mathcal{H}_{e\mu} & \mathcal{H}_{\mu\tau} \\ -\mathcal{H}_{\mu s} & -\mathcal{H}_{\tau s} & 0 & \mathcal{H}_{e\mu} & \Delta_{es} & \mathcal{H}_{e\tau} \\ 0 & -\mathcal{H}_{es} & -\mathcal{H}_{\mu s} & \mathcal{H}_{\mu\tau} & \mathcal{H}_{e\tau} & \Delta_{\tau s} \end{vmatrix} = 0 \quad (80)$$

In the limit of weak mixing with ν_s the determinant of this matrix is reduced to the product of two determinants:

$$D_6 \approx \det \begin{vmatrix} \Delta_{e\mu} & -\mathcal{H}_{\mu\tau} & \mathcal{H}_{e\tau} \\ -\mathcal{H}_{\mu\tau} & \Delta_{e\tau} & \mathcal{H}_{e\mu} \\ -\mathcal{H}_{e\tau} & \mathcal{H}_{e\mu} & \Delta_{\mu\tau} \end{vmatrix} \times \det \begin{vmatrix} \Delta_{\mu s} & \mathcal{H}_{e\mu} & \mathcal{H}_{\mu\tau} \\ \mathcal{H}_{e\mu} & \Delta_{es} & \mathcal{H}_{e\tau} \\ \mathcal{H}_{\mu\tau} & \mathcal{H}_{e\tau} & \Delta_{\tau s} \end{vmatrix} \quad (81)$$

The first term determines resonances in the active neutrino sector, while the second one determines resonances between ν_s and three active neutrinos. Of course resonances manifest themselves in the process of numerical calculations and we have checked that they are indeed in the right positions determined by the above equations.

6.1 Simplifying the problem

If we assume that active-sterile neutrino mixing is small, we can write the neutrino mixing matrix as:

$$U = \begin{pmatrix} U_{e1}^{\text{act}} & U_{e2}^{\text{act}} & U_{e3}^{\text{act}} & \eta_1 \\ U_{\mu 1}^{\text{act}} & U_{\mu 2}^{\text{act}} & U_{\mu 3}^{\text{act}} & \eta_2 \\ U_{\tau 1}^{\text{act}} & U_{\tau 2}^{\text{act}} & U_{\tau 3}^{\text{act}} & \eta_3 \\ \epsilon_1 & \epsilon_2 & \epsilon_3 & 1 \end{pmatrix} \quad (82)$$

where $U^{\text{act}} = U_{23} \cdot U_{13} \cdot U_{12}$ is the 3×3 active neutrino mixing matrix and:

$$\eta_1 = -U_{e1}^{\text{act}} \epsilon_1 - U_{e2}^{\text{act}} \epsilon_2 - U_{e3}^{\text{act}} \epsilon_3 \quad (83)$$

$$\eta_2 = -U_{\mu 1}^{\text{act}} \epsilon_1 - U_{\mu 2}^{\text{act}} \epsilon_2 - U_{\mu 3}^{\text{act}} \epsilon_3 \quad (84)$$

$$\eta_3 = -U_{\tau 1}^{\text{act}} \epsilon_1 - U_{\tau 2}^{\text{act}} \epsilon_2 - U_{\tau 3}^{\text{act}} \epsilon_3 \quad (85)$$

The previous relations are correct to first order in $\epsilon_1, \epsilon_2, \epsilon_3$ (or equivalently η_1, η_2, η_3).

We assume for simplicity that $\theta_{13} = 0$, while we take $\theta_{12} = \theta_{\text{sol}}$ and $\theta_{23} = \theta_{\text{atmo}}$. Concerning mass differences, we assume $\delta m_{21}^2 \equiv m_2^2 - m_1^2 = \delta m_{\text{sol}}^2$, and $\delta m_{32}^2 \equiv m_3^2 - m_2^2 = \delta m_{\text{atmo}}^2$. Solar and atmospheric oscillation parameters are given by eq. (1) and (2) respectively.

If $\theta_{13} = 0$, one can take advantage of the symmetry between ν_μ and ν_τ to simplify the problem. The early universe, indeed, does not distinguish between ν_μ and ν_τ at $T < m_\mu$. We can thus make a rotation in the flavor basis:

$$\begin{pmatrix} \nu_e \\ \nu'_\mu \\ \nu'_\tau \\ \nu_s \end{pmatrix} = U_{23}^{-1} \begin{pmatrix} \nu_e \\ \nu_\mu \\ \nu_\tau \\ \nu_s \end{pmatrix} \quad (86)$$

In this basis the mixing matrix becomes:

$$U' = \begin{pmatrix} \cos \theta_{12} & \sin \theta_{12} & 0 & \eta'_1 \\ -\sin \theta_{12} & \cos \theta_{12} & 0 & \eta'_2 \\ 0 & 0 & 1 & \eta'_3 \\ \epsilon_1 & \epsilon_2 & \epsilon_3 & 1 \end{pmatrix} \quad (87)$$

where:

$$\eta'_1 = \eta_1 = -\cos \theta_{12} \cdot \epsilon_1 - \sin \theta_{12} \cdot \epsilon_2 \quad (88)$$

$$\eta'_2 = \cos \theta_{23} \cdot \eta_2 - \sin \theta_{23} \cdot \eta_3 = \sin \theta_{12} \cdot \epsilon_1 - \cos \theta_{12} \cdot \epsilon_2 \quad (89)$$

$$\eta'_3 = \sin \theta_{23} \cdot \eta_2 + \cos \theta_{23} \cdot \eta_3 = \epsilon_3 \quad (90)$$

The problem which was written in terms of the parameters (η_1, η_2, η_3) can be easier treated in terms of the parameters $(\eta'_1, \eta'_2, \eta'_3 = \epsilon_3)$. By using these parameters, it can be easily separated into two smaller sub-problems. In the following sections, we will discuss separately the constraint on η'_3 and (η'_1, η'_2) . In the final section we will combine our results.

6.2 Bounds on η'_3

The bounds on $\eta'_3 = \epsilon_3$ can be immediately obtained from the results of section 4, since this is a pure “1 active + 1 sterile neutrino” problem. Clearly the result depends on the value of the mass difference

$$\delta m_{43}^2 = m_4^2 - m_3^2. \quad (91)$$

When $\delta m_{43}^2 \geq 0$ active-sterile transitions are non-resonant. As a consequence, eq. (39) (and subsequent discussion) is valid. In terms of η'_3 we have thus:

$$(\delta m_{43}^2 / \text{eV}^2) (2\eta'_3)^4 = 1.74 \cdot 10^{-5} \ln^2(1 - \Delta N_\nu) \quad (92)$$

When $\delta m_{43}^2 < 0$, sterile neutrino production occurs through resonant transitions. This means that eq. (57) (and subsequent discussion) is approximatively valid. With very simple algebra, assuming that the number of extra neutrinos ΔN_ν is approximatively given by the sterile neutrino energy density, we can obtain the following relation:

$$(|\delta m_{43}^2| / \text{eV}^2) (2\eta'_3)^4 = 1.9 \cdot 10^{-9} \ln^2(1 - \Delta N_\nu) \quad (93)$$

We remark that the two equations above take into account only sterile neutrino production, while they do not consider the effects related to depletion of other neutrino flavors. As a consequence, they are quite accurate for large mass differences, while they generally underestimate the effect on BBN at smaller masses (since they neglect effects of ν_e depletion on $n - p$ transformations). More precise bounds can be read from fig. 1 and 5 with the identification $\delta m^2 \rightarrow \delta m_{43}^2$ and $\sin^2(2\theta) \rightarrow (2\eta'_3)^2$.

6.3 Bounds on η'_1 and η'_2

The problem described by the parameters (η'_1, η'_2) is much more complicated since it involves directly two active and one sterile neutrino, with mixing described by:

$$\begin{pmatrix} \nu_e \\ \nu'_\mu \\ \nu'_\tau \\ \nu_s \end{pmatrix} = \begin{pmatrix} \cos \theta_{12} & \sin \theta_{12} & 0 & \eta'_1 \\ -\sin \theta_{12} & \cos \theta_{12} & 0 & \eta'_2 \\ 0 & 0 & 1 & 0 \\ \epsilon_1 & \epsilon_2 & 0 & 1 \end{pmatrix} \begin{pmatrix} \nu_1 \\ \nu_2 \\ \nu_3 \\ \nu_4 \end{pmatrix} \quad (94)$$

The mixing angle θ_{12} and the mass difference δm_{21}^2 are fixed by KamLAND and by solar neutrino experiments, see eqs. (1).

It is very difficult to obtain analytic estimates in the general case. However, one can simply understand what happen in the limiting cases. Let us consider the situation $m_4 \gg m_2 > m_1$ (or $m_4 \ll m_1 < m_2$). In this case, we can approximatively neglect the mass difference δm_{21}^2 . The angle θ_{12} can thus be rotated away, resulting in:

$$\begin{pmatrix} \nu_e \\ \nu'_\mu \\ \nu'_\tau \\ \nu_s \end{pmatrix} = \begin{pmatrix} 1 & 0 & 0 & \eta'_1 \\ 0 & 1 & 0 & \eta'_2 \\ 0 & 0 & 1 & 0 \\ \eta'_1 & \eta'_2 & 0 & 1 \end{pmatrix} \begin{pmatrix} \nu_1 \\ \nu_2 \\ \nu_3 \\ \nu_4 \end{pmatrix} \quad (95)$$

By repeating the discussion of the previous section, one obtains then:

$$(\delta m_{41}^2/\text{eV}^2) (2\eta'_1)^4 = 3.16 \cdot 10^{-5} \ln^2(1 - \Delta N_\nu) \quad (96)$$

$$(\delta m_{42}^2/\text{eV}^2) (2\eta'_2)^4 = 1.74 \cdot 10^{-5} \ln^2(1 - \Delta N_\nu) \quad (97)$$

where we assumed positive mass differences, i.e. $\delta m_{41}^2 \simeq \delta m_{42}^2 \gg \delta m_{21}^2 > 0$. When mass differences are negative, i.e. $\delta m_{41}^2 \simeq \delta m_{42}^2 \ll -\delta m_{21}^2 < 0$, one expect instead

$$(|\delta m_{41}^2|/\text{eV}^2) (2\eta'_1)^4 = 5.2 \cdot 10^{-10} \ln^2(1 - \Delta N_\nu) \quad (98)$$

$$(|\delta m_{42}^2|/\text{eV}^2) (2\eta'_2)^4 = 1.9 \cdot 10^{-9} \ln^2(1 - \Delta N_\nu) \quad (99)$$

The other limiting situation that we can understand analytically is $m_2 \gg m_4 \simeq m_1$. In this case we can approximatively neglect the mass difference δm_{41}^2 . The mixing in the (1-4)-sector can thus be re-absorbed, leading to:

$$\begin{pmatrix} \nu_e \\ \nu'_\mu \\ \nu'_\tau \\ \nu_s \end{pmatrix} = \begin{pmatrix} \cos \theta_{12} & \sin \theta_{12} & 0 & 0 \\ -\sin \theta_{12} & \cos \theta_{12} & 0 & \varphi \\ 0 & 0 & 1 & 0 \\ \varphi \cdot \sin \theta_{12} & -\varphi \cdot \cos \theta_{12} & 0 & 1 \end{pmatrix} \begin{pmatrix} \nu_1 \\ \nu_2 \\ \nu_3 \\ \nu_4 \end{pmatrix} \quad (100)$$

where:

$$\varphi = \eta'_1 \cdot \tan \theta_{12} + \eta'_2 = -\epsilon_2 / \cos(\theta_{12}) \quad (101)$$

We can see that the mixing between active and sterile neutrinos is described by a parameter φ . If $\varphi \neq 0$, a resonant transitions occur among ν_s and ν'_μ . This mechanism should dominate the production of sterile neutrinos. As a consequence, we expect the following relation to be valid:

$$(|\delta m_{42}^2|/\text{eV}^2) (2\varphi \cdot \cos(\theta_{12}))^4 = 1.9 \cdot 10^{-9} \ln^2(1 - \Delta N_\nu) \quad (102)$$

where φ is given as a function of η'_1 and η'_2 by eq. (101) ⁶.

In order to check the validity of the previous conclusions and to have a better understanding of the BBN bounds on sterile neutrinos, we solved numerically kinetic equations, varying, one at a time, the parameter η'_1 and η'_2 . As a first step, we considered the situation

⁶We note that the parameters η'_1 and η'_2 can be chosen in principle in such a way that $\varphi = 0$. When $\varphi = 0$, sterile neutrinos are not mixed with active ones and we should expect that sterile neutrinos are not produced. In reality, this result simply indicates that, in the limit considered ($m_2 \gg m_4 \simeq m_1$), no effects driven by the dominant mass difference, δm_{21}^2 are expected. Even in this case, however, sterile neutrinos can in principle be produced, due to oscillation driven by sub-dominant mass differences δm_{41}^2 .

when the mixing matrix U can be written as $U = U_{24} \cdot U_{12}$, with δm^2_{21} and θ_{12} fixed at solar values, see eq. (1). It is evident that, in the limit of small mixing, one has $\theta_{24} \simeq \eta'_2$. The results obtained are shown, as functions of δm^2_{42} and $\sin^2(\theta_{24})$, in figs. 7 (for the case $\delta m^2_{42} > 0$) and in figs. 8 (for the case $\delta m^2_{42} < 0$). Red dotted lines correspond to analytic estimates which are obtained from eq. (97) in the case of positive δm^2_{42} and from eq. (99) in the case of negative δm^2_{42} . One can see that there is a good agreement with numerical calculations for large values of mass difference. For small values of $|\delta m^2_{42}|$ agreement is less satisfactory (especially for $\delta m^2_{42} < 0$) both because the analytic estimates, derived for the limiting behaviours, are less appropriate and because depopulation of electron neutrinos becomes relevant. In particular, by comparing figs. 7 and 8 with figs. 1 and 5 (which show the results obtained when we neglect the mixing U_{12}), one can see that generally the effect of mixing between active neutrinos is to increase ν_e depletion, with the consequence of a stronger bound on the active-sterile mixing.

Similar conclusions can be obtained from figs. 9 and 10. In these figures we show numerical results for the situation in which the mixing matrix U can be written as $U = U_{14} \cdot U_{12}$. In the limit of small mixing angle one has $\theta_{14} \simeq \eta'_1$. Analytic estimates (red dotted lines) are obtained from eq. (96) for $\delta m^2_{41} \geq \delta m^2_{21}$, from eq. (102) for $0 < \delta m^2_{41} < \delta m^2_{21}$ and from eq. (98) for $\delta m^2_{41} < 0$. One sees that there is a good agreement between numerical calculations and analytical estimates. In all the cases, analytic estimates underestimate the BBN bounds on active sterile mixing.

6.4 Combining results

As a summary, by considering variations of the parameter $\eta'_3 = \epsilon_3$, we have obtained:

$$(\delta m^2_{43}/\text{eV}^2) (2\eta'_3)^4 = 1.74 \cdot 10^{-5} \ln^2(1 - \Delta N_\nu) \quad \text{for } m_4 \geq m_3 \quad (103)$$

$$(|\delta m^2_{43}|/\text{eV}^2) (2\eta'_3)^4 = 1.9 \cdot 10^{-9} \ln^2(1 - \Delta N_\nu) \quad \text{for } m_4 < m_3 \quad (104)$$

These relations are approximate and generally underestimate the effect on BBN at small masses. More precise bounds can be read from fig. 5 with the identification $\delta m^2 \rightarrow \delta m^2_{43}$ and $\sin^2(2\theta) \rightarrow (2\eta'_3)^2$.

By considering variations, one at a time, of η'_1 and η'_2 we have obtained:

$$\begin{aligned} (\delta m^2_{41}/\text{eV}^2) (2\eta'_1)^4 &= 3.16 \cdot 10^{-5} \ln^2(1 - \Delta N_\nu) \\ (\delta m^2_{42}/\text{eV}^2) (2\eta'_2)^4 &= 1.74 \cdot 10^{-5} \ln^2(1 - \Delta N_\nu) \\ &\text{for } m_4 \geq m_2 > m_1 \end{aligned} \quad (105)$$

$$\begin{aligned} (|\delta m^2_{42}|/\text{eV}^2) [2(\eta'_1 \sin(\theta_{12}) + \eta'_2 \cos \theta_{12})]^4 &= 1.9 \cdot 10^{-9} \ln^2(1 - \Delta N_\nu) \\ &\text{for } m_2 \geq m_4 > m_1 \end{aligned} \quad (106)$$

$$\begin{aligned} (|\delta m^2_{41}|/\text{eV}^2) (2\eta'_1)^4 &= 5.2 \cdot 10^{-10} \ln^2(1 - \Delta N_\nu) \\ (|\delta m^2_{42}|/\text{eV}^2) (2\eta'_2)^4 &= 1.9 \cdot 10^{-9} \ln^2(1 - \Delta N_\nu) \\ &\text{for } m_2 > m_1 > m_4 \end{aligned} \quad (107)$$

As above, these constraints are approximate and more precise bounds can be read from figs. 7,8,9,10.

In general scenario all parameters are possibly different from zero at the same time and the effects described above are all observed together. We do not expect, however, strong compensations to occur because the described effects have generally different magnitude

and because, in terms of the parameter $(\eta'_1, \eta'_2, \eta'_3)$, the problem is well separated in nearly all range of possible masses (except for $m_2 \geq m_4 > m_1$). This means that the bounds on $(\eta'_1, \eta'_2, \eta'_3)$ can be translated into constraints on (η_1, η_2, η_3) and $(\epsilon_1, \epsilon_2, \epsilon_3)$. We remind that $\eta = U_{23} \cdot \eta'$ and $\epsilon = -(U_{12})^{-1} \cdot \eta'$.

7 Non-vanishing lepton asymmetry

We assumed above that lepton asymmetry of cosmological plasma is either very small or has the natural value, $\eta \sim 10^{-9}$, of the same order of magnitude as cosmological baryon asymmetry. The charge asymmetric contribution to neutrino effective potential in plasma (eq. (10)) is

$$V^{(asym)} = 1.1 \cdot 10^{-20} (\eta^{(a)} / 10^{-9}) / x^3 \quad (108)$$

Thus one can see that for such η the Hamiltonian (9) is either dominated by the mass difference term (at low temperatures $T = 1/x$) or by the non-local one (at high temperatures). However the magnitude of lepton asymmetry of neutrinos can be much larger than 10^{-9} either due to resonance rise of the asymmetry because of charge asymmetric transformation of ν_a into ν_s and $\bar{\nu}_a$ into $\bar{\nu}_s$ [22, 33] or due to primordially generated large lepton asymmetry. There are plenty cosmological scenarios leading simultaneously to small baryon asymmetry and to much larger, even of order unity, lepton asymmetry [34]. In both cases neglected up to this point charge asymmetric contribution into V_{aa} (10) could become dominant.

The best bounds on the values of the lepton asymmetry can be found from BBN, see review [20]. These bounds have been considerably improved due to strong mixing between active neutrinos [27, 35]. It allows to put the upper bound on the common chemical potential of all neutrino species

$$|\xi_a| = |\mu_a/T| < 0.07 \quad (109)$$

This limit is loose enough to allow the charge asymmetric part of the potential to play a significant role in neutrino oscillations in the early universe. An analysis of BBN with non-zero chemical potentials and possible active-sterile neutrino mixing has been performed recently in ref. [21].

Let us first consider naturally small initial value of $\eta \leq 10^{-9}$ and later more questionable larger values of primordial lepton asymmetry. For small asymmetry and positive mass difference between ν_s and any active neutrino MSW-resonance would not be efficient (see below eq. (122)). Hence lepton asymmetry would remain always small and $V^{(asym)}$ (108) may be neglected. Thus the bounds obtained above in non-resonance case are justified. This may be not so if mass difference is negative and the resonance transition between ν_s and ν_a could take place. As a result a large lepton asymmetry, close to or even a little larger than $\eta = 0.1$, can be generated in the active neutrino sector [22, 33]. Of course the total leptonic charge of active plus sterile neutrinos is conserved and a lepton asymmetry of active neutrinos is compensated by opposite sign of lepton asymmetry of ν_s . Neglecting $V^{(asym)}$ in this case would be unreasonable. However, as we see below, a large lepton asymmetry can be generated only for very small values of mixing angle between ν_s and ν_a :

$$\sin^4 2\theta |\delta m^2| < \begin{cases} 10^{-9} & \text{for } \nu_e \\ 3 \times 10^{-9} & \text{for } \nu_{\mu, \tau} \end{cases} \quad (110)$$

Here mass difference is measured in eV^2 . Note that the bound for ν_e is stronger than for $\nu_{\mu, \tau}$, in contrast to the bounds (38), (39). For the values of parameters outside this region the

approach used above (with $V^{(asym)}$ neglected) is justified. As we have seen in the previous sections, the allowed interval of $(\theta - \delta m^2)$ found in the resonance case but without $V^{(asym)}$, is inside the parameter space restricted by (110). Hence we can conclude that the area outside of (110) is definitely excluded and that the real bound can be stronger. It is more difficult to make conclusion about allowed range of the mixing parameters inside the region (110) because an excessive number of neutrino species may be compensated by electronic charge asymmetry. However, one should take into account that the generated lepton asymmetry could be strongly inhomogeneous [36] (see also [20, 37]). If the mixing angle is larger than 10^{-4} , so that the lepton asymmetry in the minimum (see below discussion after eq. (117)) drops more than by 5 orders of magnitude, then the universe would consist of chaotic domains with equal positive and negative values of η [20] and the impact of the electronic lepton asymmetry on BBN would be less pronounced after averaging over such domains. On the other hand, as argued in ref. [37], production of sterile neutrinos on very steep domain walls might be resonance enhanced and it may lead to unacceptable large ΔN_ν . The problem is not yet settled down and deserves more investigation.

Anyhow, even the limit (110), which allows the resonance generation of lepton asymmetry is quite strong, much stronger than the non-resonant one and, for $|\delta m^2| > 10^{-4}$, it is also stronger than the limits obtained in direct measurements.

Resonance rise of lepton asymmetry does not take place in the case of strong $(\nu_s - \nu_a)$ -mixing by the following evident reason. If mixing is large both active and sterile neutrinos quickly reach thermal equilibrium when charge asymmetry is vanishing, $\rho_{aa} = \bar{\rho}_{aa} = \rho_{ss} = \bar{\rho}_{ss} = f_{eq}$. To find the magnitude of mixing angle when fast equilibration takes place we will use analytical calculations of ref. [33]. The evolution of the charge asymmetry is governed by the following equation derived in the limit of large values of parameters $K_a \gg 1$:

$$\frac{dZ_a(q)}{dq} = \frac{10^{10} K_a^2 (\sin 2\theta)^2}{16\pi^2} \int_0^\infty dy f_{eq}(y) \int_{q_{in}}^q dq_1 \Sigma(q_1, y) \exp \left[-\frac{\epsilon_a y \zeta}{qq_1} \right] \sin \left[\zeta \left(\frac{1}{y} - \frac{y}{qq_1} \right) \right] \sin \left[b_a K_a \int_{q_1}^q dq_2 \frac{Z_a(q_2)}{q_2^{4/3}} \right] \quad (111)$$

where $\zeta = K_a(q - q_1)$ is effectively integration variable and the constants depending upon the active neutrino flavor are given by:

$$K_e = 5.63 \cdot 10^4 (|\delta m^2| \cos 2\theta)^{1/2}, \quad K_{\mu, \tau} = 2.97 \cdot 10^4 (|\delta m^2| \cos 2\theta)^{1/2}, \quad (112)$$

$$b_e = 3.3 \cdot 10^{-3} (|\delta m^2| \cos 2\theta)^{-1/3}, \quad b_{\mu, \tau} = 7.8 \cdot 10^{-3} (|\delta m^2| \cos 2\theta)^{-1/3}, \quad (113)$$

$$\epsilon_e \approx 7.4 \cdot 10^{-3}, \quad \epsilon_{\mu, \tau} \approx 5.2 \cdot 10^{-3}. \quad (114)$$

The quantity Z is related to charge asymmetry of active neutrinos as

$$Z_a = 1.67 \cdot 10^9 \eta_a \quad (115)$$

and the new “time” variable q is chosen in such a way that in the limit of small charge asymmetry the resonance always takes place at $q = y$, i.e. $q = \beta_a x^3$ with

$$\beta_e = 6.63 \cdot 10^3 (|\delta m^2| \cos 2\theta)^{1/2}, \quad \beta_{\mu, \tau} = 1.257 \cdot 10^4 (|\delta m^2| \cos 2\theta)^{1/2}. \quad (116)$$

The function $\Sigma(q, y)$ is given by

$$\Sigma = \rho_{aa} + \bar{\rho}_{aa} - \rho_{ss} - \bar{\rho}_{ss} \quad (117)$$

Equation (111) was solved in ref. [33] under assumption that Σ varies very slowly and in an essential interval of q it is approximately equal to its initial value, $\Sigma_{in} = 2$. This approximation is valid for sufficiently small mixing angle θ and we will determine below when it is true. For small q the charge asymmetry Z exponentially decreases and only for $q > 1.278$ it starts to rise. For $\sin 2\theta = 10^{-4}$ and $\delta m^2 = 1 \text{ eV}^2$ the asymmetry drops by 3 orders of magnitude, for larger θ the decrease would be much stronger.

In the limit of small charge asymmetry Σ satisfies the equation (in this equation and below we will omit sub-indices a):

$$\frac{d\Sigma}{dq} = - \left(\frac{K \sin^2 2\theta}{y} \right)^2 \int_{q_{in}}^q dq_1 \Sigma(q_1, y) \exp \left[-\frac{\epsilon y \zeta}{qq_1} \right] \cos \left[\zeta \left(\frac{1}{y} - \frac{y}{qq_1} \right) \right] \quad (118)$$

For large K the integral in the r.h.s. “sits” on the upper limit and can be easily taken. Thus we come to the equation:

$$\frac{d\Sigma}{dq} = - \frac{K \epsilon y q^2 \sin^2 2\theta}{(q^2 - y^2) + \epsilon^2 y^4} \Sigma \quad (119)$$

The solution of this equation is straightforward. It can be substituted into eq. (111) and we find that asymmetry does not rise if Σ quickly decreases. According to this solution, this happens if the mixing is bounded from below as given by eq. (110).

Let us now consider the case of a large *primordial* lepton asymmetry and check if a stronger mixing between active and sterile neutrinos is allowed. If so, then an experimental discovery of mixing between ν_a violating the bounds derived above would indicate that the cosmological lepton asymmetry is much larger than the baryonic one or that neutrinos possess a new interaction, as e.g. coupling to Majorons, which might strongly change the oscillation behavior in cosmological plasma [38].

If the contribution of the lepton asymmetry into neutrino effective potential (10) is non-negligible, then resonance transition would exist for any sign of mass difference. In both cases, there are two resonances but for $\delta m^2 > 0$ these two resonances are either in neutrino or antineutrino channels (depending on the sign of η), while for $\delta m^2 < 0$ there is one resonance in neutrino channel and one resonance in antineutrino channel. We assume that the mixing is sufficiently weak, so only the resonance transitions are of importance. The resonance condition looks as following:

$$5 \cdot 10^{-13} c_2 \delta m^2 \frac{x}{y} + 10^{-20} \kappa_a \frac{y}{x^5} \pm 1.1 \cdot 10^{-20} \eta_9 \frac{1}{x^3} = 0 \quad (120)$$

where $c_2 = \cos 2\theta$, $\kappa_e = 1.137$, $\kappa_{\mu, \tau} = 0.317$, $\eta_9 = 10^9 \eta$, the signs \pm refer to antineutrino (+) and neutrino (−) respectively. Solving this equation we find the resonance values of neutrino momentum:

$$y_{1,2} = \pm (0.55/\kappa) \eta_9 x^2 \left(1 \pm \sqrt{1 - \lambda x^2} \right) \quad (121)$$

where $\lambda = 1.65 \cdot 10^8 c_2 \kappa \delta m^2 / \eta_9^2$.

If $\delta m^2 > 0$, i.e. ν_s is heavier than active neutrinos, then the resonances occur only for $\lambda x^2 < 1$. The oscillations could have an impact on BBN if they are efficient in the interval $x = 0.1 - 2$. Hence the charge asymmetry should be sufficiently large:

$$\eta_9 > 1.3 \cdot 10^4 c_2^{1/2} \kappa^{1/2} (\delta m^2)^{1/2} \quad (122)$$

We can roughly estimate resonance contribution into production of sterile neutrinos integrating eq. (36) over y with $\rho_{ss} \ll \rho_{aa} = f_{eq}$:

$$\frac{d}{dx} \left(\frac{n_s}{n_{eq}} \right) = 2.45 \cdot 10^{16} \kappa^{-1} s_2^2 c_2 (\delta m^2)^2 x^8 \frac{y_1 \exp(-y_1) + y_1 \exp(-y_1)}{y_1 - y_2} \quad (123)$$

where $s_2 = \sin 2\theta$. Equation (36) gives a good description of the ν_s production rate also in the resonance case if the mass difference is not too small. As we have mentioned above, both resonances are effective either in $(\nu_a - \nu_s)$ -transition (for $\eta > 0$) or in $(\bar{\nu}_a - \bar{\nu}_s)$ -transition (for $\eta < 0$). Hence resonance transitions diminish the absolute value of the original asymmetry. Indeed, if e.g. the resonances operate in $\nu_a \leftrightarrow \nu_s$ channel the transition of ν_a into ν_s would be more efficient than the charge conjugated transition of $\bar{\nu}_a$ into $\bar{\nu}_s$ and the number difference between ν_a and $\bar{\nu}_a$ would decrease. If the resonance took place above $T = 3 - 5$ MeV (or at x below $x = 0.33 - 0.2$), then the distribution of ν_a and $\bar{\nu}_a$ would have equilibrium form with chemical potentials satisfying $\xi_a = -\bar{\xi}_a$ and the standard BBN code can be applied to calculations of light element production. For smaller resonance temperatures chemical equilibrium would not be restored and thus $\xi_a \neq -\bar{\xi}_a$. The code should be modified to include this effect.

Let us find now what is the largest possible value of the lepton charge asymmetry η allowed by the limit (109):

$$\eta = \frac{n_\nu - n_{\bar{\nu}}}{n_\gamma} = \frac{3}{11} \frac{\pi^2/6}{1.8} \xi = 0.25 \xi \quad (124)$$

where the first factor $3/11$ comes from the present day neutrino-to-photon number ratio and the second one comes from the ratio of the equilibrium number densities $(n_\nu - n_{\bar{\nu}})/(n_\nu + n_{\bar{\nu}})$. The result is valid in the limit of small ξ . Since individual chemical potentials before equilibration enforced by $\nu_e - \nu_\mu - \nu_\tau$ oscillations may be at most three times larger than the limiting value $|\xi| = 0.07$ we conclude that the maximum magnitude of the primordial lepton asymmetry is $\eta = 0.05$. Another formally open possibility is large values of $2\eta_{\nu_e} + \eta_{\nu_\mu} + \eta_{\nu_\tau}$ and/or of $2\eta_{\nu_\mu} + \eta_{\nu_e} + \eta_{\nu_\tau}$ (and $\mu \leftrightarrow \tau$), contributing into effective potential of different neutrino species but a strong compensation in the sum $\xi_e + \xi_\mu + \xi_\tau$ down to 0.2.

If we take $\eta = 0.05$ then the contribution of the first resonance is strongly suppressed and only the second resonance corresponding to smaller y is effective. The produced ν_s would contribute to the additional number of neutrino species as:

$$\Delta N_\nu = 0.8 \cdot 10^9 s_2^2 (\delta m^2)^3 \int_0^{x_{max}} dx x^{10} \exp[-0.9 \delta m^2 x^4] \quad (125)$$

where it was assumed that $c_2 = 1$. As an upper limit of integration we will take $x_{max}^{(e)} = 0.3$ in accordance with the estimates presented after eq. (17). If we mixing would be predominantly with ν_μ or ν_τ one should seemingly take $x_{max}^{(\mu, \tau)} = 0.2$. However this is not so because refilling of active neutrino species would take place through $e^+ e^- \rightarrow \nu_e \bar{\nu}_e$ with subsequent fast transformation of ν_e into ν_μ and ν_τ through oscillations and hence one should take $x_{max}^{(\mu, \tau)} = x_{max}^{(e)} = 0.3$.

If the mass difference is smaller than $\delta m_{max}^2 \sim 10^2 \text{ eV}^2$ (notice that cosmological limits on masses of active neutrinos [20] are not applicable to ν_s because their number density may be much smaller than the equilibrium one) then $\exp[-0.9 \delta m^2 x^4] \approx 1$ and we obtain

$$\Delta N_\nu = 7 \cdot 10^7 s_2^2 (\delta m^2)^3 x_{max}^{11} \approx 10^2 s_2^2 (\delta m^2)^3 \quad (126)$$

If $s_2 \sim 0.1$ then the oscillations could diminish primordial lepton asymmetry of active neutrinos and produce noticeable amount of ν_s .

However a more important for BBN effect comes from larger x . Above $x = 0.3$ refilling of neutrino states may be neglected and the total number/energy density of $\nu_e + \nu_\mu + \nu_\tau + \nu_s$ would be constant. Correspondingly production of sterile neutrino states would lead to an equal decrease of active ones. Due to strong mixing between the later the deficit of active neutrinos would be equally distributed between all three active species. As we have discussed above, BBN is very sensitive to a deficit of ν_e . We estimate the ν_s production using eq. (125) with $x_{max} = 1.4$, i.e. inverse temperature of neutron-proton freezing. For $\delta m^2 = 1 \text{ eV}^2$ we obtain $\Delta N_{\nu_s} = 3 \times 10^8 s_2^2$ and for small δm^2 , such that $\delta m^2 x^4 < 1$, $\Delta N_{\nu_s} = 3 \times 10^9 s_2^2 (\delta m^2)^3$. The deficit of ν_e (or $\bar{\nu}_e$, depending on the sign of initial η) would be equal to one third of that. However there is one more twist, namely there was some primordial lepton asymmetry of active neutrinos and oscillations between ν_a and ν_s would diminish the absolute magnitude of the latter. As a result we could arrive to (almost) equal number densities of active neutrinos and antineutrinos which would be suppressed with respect to the standard one by the factor $\exp[-|\sum_a \xi_a^{(in)}|/3]$ where $\xi_a^{(in)}$ are primordial values of chemical potentials of active neutrinos. According to eq. (28), a deficit of ν_e and equal deficit of $\bar{\nu}_e$ is equivalent to addition of $\Delta N_\nu = 12.3|\xi|$. In this way we obtain essentially the same bound as eq. (109). However, it is not so in a general case. Invoking an additional parameter, the value of primordial lepton asymmetry, evidently makes the bounds on mixing between ν_s and ν_a less restrictive as well as the bounds on the value of lepton asymmetry obtained from BBN in absence of mixing with ν_s .

Now let us consider negative mass difference, $\delta m^2 < 0$, when resonance is possible even with vanishingly small charge asymmetry. Since active neutrinos are assumed to be heavier than ν_s the mass difference is bounded by the recent WMAP data [40] by $\delta m^2 < 0.06 \text{ eV}^2$. In this case, of negative δm^2 , there are again two resonances but now one is in neutrino channel, while the other is in antineutrino channel, as can be seen from eq. (121) with $\lambda < 0$. If the initial value of $|\eta|$ is sufficiently large, then $|\eta|$ would rise as a result of oscillations between ν_a and ν_s in contrast to positive mass difference, $\delta m^2 > 0$, when oscillations lead to a decrease of $|\eta|$.

The rate of transformation of ν_a into ν_s and of the charged conjugated process can be found from equation which is similar to eq. (123) where only one resonance is effective. For a positive lepton asymmetry, $\eta > 0$, the resonance in neutrino channel takes place at $y = y_1$ (with positive sign of the square root) and the resonance in antineutrino channel takes place at $y = y_2$. For a large and, say, positive η the resonance in neutrino channel is too far, $y_1 \gg 1$, in the essential range of x and its contribution can be neglected - this is similar to the discussed above case of positive δm^2 . The resonance in antineutrino channel takes place at $y_2 \sim (4.5 \cdot 10^7 / \eta_9) x^4$ and could efficiently transform $\bar{\nu}_a$ into $\bar{\nu}_s$. It would lead to an increase of η . For a more accurate calculation of the transformation rate one should include non-vanishing chemical potential into number density of active neutrinos in eq. (36), $\rho_{aa} = f_{eq} = \exp(-y + \xi)$ but since we usually consider small $\xi \ll 1$, this correction is not of much importance. The oscillations create an increase of the absolute value of the lepton asymmetry and hence the BBN bounds on the initial magnitude of the latter should be generally stronger than in no-oscillation case. However there are several effects “working” in the opposite direction which may compensate each other and so the bounds on η for concrete values of the oscillation parameters in each case should be derived separately. It can be approximately done using results presented in this section.

8 Conclusion

We have shown above that the effects of strong mixing between all three active neutrinos noticeably change the BBN bounds on the possible admixture of sterile neutrinos previously obtained under assumption of no active-active mixing. Our results are summarized in sec. 6 with simple analytical expressions. They essentially depend upon the sign of mass difference between different neutrino species, because the latter determines the number and positions of the resonances. More detailed and more accurate bounds can be read-off from figures 1,5,7,8,9,10, panel 4 in all the cases. The results depend upon the limits on the number of effective neutrino flavors allowed by BBN. One can see that even with very modest limits there is not much freedom permitted to admixture of sterile neutrinos to the known active ones.

If lepton asymmetry of the universe is non-negligible the conclusions are less definite because of the additional parameter, the value of the asymmetry. However, if asymmetry is generated by the oscillations themselves, the mixing with ν_s should be very small, below the bounds derived for the case of vanishing asymmetry. For the case of primordial asymmetry the bounds are weaker and with some conspiracy they could be very weak, allowing rather strong mixing between sterile and active neutrinos. More detailed investigation is desirable in this case.

Acknowledgment A.D. Dolgov is grateful to the Research Center for the Early Universe of the University of Tokyo for the hospitality during the time when this work was completed. F.L. Villante is grateful to A. Mirizzi, D. Montanino, M. Giannotti and D. Comelli for useful suggestions and comments.

References

- [1] SNO Collaboration, Phys. Rev. Lett. 89 (2002) 011301; Phys. Rev. Lett. 89 (2002) 011302.
- [2] KamLAND Collaboration, Phys. Rev. Lett. 90 (2003) 021802.
- [3] S. Fukuda *et al.*, Super-Kamiokande Coll., Phys. Lett. B539 (2002) 179;
B.T. Cleveland *et al.*, Astrophys. J. 496, 505 (1998);
D.N. Abdurashitov *et al.*, SAGE Coll., Phys. Rev. C60, 055801 (1999); astro-ph/0204245;
W. Hampel *et al.*, GALLEX Coll., Phys. Lett. B447, 127 (1999);
C. Cattadori, GNO Coll., Nucl. Phys. B (Proc. Suppl.) 110 (2002) 311.
- [4] Super-Kamiokande Coll., Y. Fukuda *et al.*, Phys. Rev. Lett. 81 (1998) 1562;
MACRO Coll., M. Ambrosio *et al.*, Phys. Lett. B434 (1998) 451.
- [5] G.L. Fogli, E. Lisi, A. Marrone, D. Montanino, A. Palazzo, A.M. Rotunno
- [6] M. Maltoni, T. Schwetz, J.W.F. Valle, hep-ph/0212129;
M. Maltoni, T. Schwetz, M.A. Tortola, J.W.F. Valle, hep-ph/0209368, Nucl. Phys. Proc. Suppl. 114 (2003) 203.
- [7] A. Bandyopadhyay, S. Choubey, R. Gandhi, S. Goswami, D.P. Roy, hep-ph/0212146.
- [8] J.N. Bahcall, M. C. Gonzalez-Garcia, C. Pena-Garay, JHEP02(2003)009.

- [9] H.Nunokawa, W.J.C. Teves, R.Z. Funchal, hep-ph/0212202.
- [10] P. Aliani, V. Antonelli, M. Picariello, E. Torrente-Lujan, hep-ph/0212212.
- [11] P.C. de Holanda, A.Yu. Smirnov, hep-ph/0212270; hep-ph/0211264.
- [12] A.Yu. Smirnov, Invited talk given at the 11th workshop on Neutrino Telescopes, Venice, March 11- 14, 2003; hep-ph/0305106.
- [13] A. Aguilar *et al.*, LSND Coll., Phys. Rev. D 64 (2001) 112007.
- [14] R. Barbieri, A.D. Dolgov, Phys. Lett. B 237 (1990) 440.
- [15] K. Enqvist, K. Kainulainen, J. Maalampi, Phys. Lett. B 244 (1990) 186.
- [16] K. Kainulainen, Phys. Lett. B 244 (1990) 191.
- [17] R. Barbieri, A.D. Dolgov, Nucl. Phys. B 349 (1991) 743.
- [18] K. Enqvist, K. Kainulainen, J. Maalampi, Nucl. Phys. B 349 (1991) 754.
- [19] K. Enqvist, K. Kainulainen, M. Thomson, Nucl. Phys. B373 (1992) 498.
- [20] A.D. Dolgov, Phys. Rept. 370 (2002) 333.
- [21] P. Di Bari, Phys. Rev. D65 (2002) 043509;
P. Di Bari, astro-ph/0302433.
- [22] R. Foot, M.J. Thomson, R.R. Volkas, Phys. Rev. D53 (1996) 5349;
R. Foot, R.R. Volkas, Phys. Rev. D55 (1997) 5147;
N. Bell, R. Foot, R.R. Volkas, Phys. Rev. D58 (1998) 105010;
P. Di Bari, R. Foot, Phys. Rev. D **65** (2002) 045003.
- [23] A.D. Dolgov, Yad.Fiz. **33** (1981) 1309; English translation: Sov. J. Nucl. Phys. **33** (1981) 700;
M.A. Rudzsky, Astrophys. Space Sci. 165 (1990) 65;
G. Sigl and G. Raffelt, Nucl. Phys. B **406** (1993) 423;
B.H.J. McKellar and M.J. Thomson, Phys. Rev. D **49** (1994) 2710.
- [24] D. Nötzold and G. Raffelt, Nucl. Phys. B307 (1988) 924.
- [25] J. Pantaleone, Phys. Lett. B287 (1992) 128.
- [26] S. Pastor, G.G. Raffelt, D.V. Semikoz, Phys. Rev. D65 (2002) 05301.
- [27] A.D. Dolgov, S.H. Hansen, S. Pastor, S.T. Petcov, G.G. Raffelt, D.V. Semikoz, Nucl.Phys. B632 (2002) 363.
- [28] A. Friedland, C. Lunardini, hep-ph/0304055.
- [29] A.D. Dolgov, S.H. Hansen, S. Pastor, D.V. Semikoz, Astropart. Phys. 14 (2000) 79.
- [30] A.D. Dolgov, hep-ph/0208222, lectures presented at ITEP Winter School, February, 2002.
- [31] A.D. Dolgov, Phys. Lett. B506 (2001) 7.

- [32] D.P. Kirilova, M.V. Chizhov, Phys. Lett. B **393** (1997) 375;
D.P. Kirilova, M.V. Chizhov, Phys. Rev. D **58** (1998) 073004;
D.P. Kirilova, M.V. Chizhov, Nucl. Phys. B **591** (2000) 457;
D. Kirilova, M. Chizhov, Nucl. Phys. Proc. Suppl. 100 (2001) 360.
- [33] A.D. Dolgov, Nucl. Phys. B610 (2001) 411.
- [34] J.A. Harvey, E.W. Kolb, Phys. Rev., D24 (1981) 2090;
A.D. Dolgov, D.K. Kirilova, J. Moscow Phys. Soc. 1, (1991), 217;
A.D. Dolgov, Phys. Repts, 222 (1992) No. 6;
A. Casas, W.Y. Cheng, G. Gelmini, Nucl. Phys. B538 (1999) 297;
J. March-Russell, A. Riotto, H. Murayama, JHEP, 11 (1999) 015;
J. McDonald, Phys. Rev. Lett. 84 (2000) 4798;
M. Kawasaki, F. Takahashi, M. Yamaguchi, Phys. Rev. D66 (2002) 043516.
- [35] C. Lunardini, A. Yu. Smirnov, Phys. Rev. D64 (2001) 073006;
Y.Y.Y. Wong, Phys. Rev. D66 (2002) 025015;
K.N. Abazajian, J.F. Beacom, N.F. Bell, Phys. Rev. D66 (2002) 013008.
- [36] P. Di Bari, Phys. Lett. B 482 (2000) 150.
- [37] K. Enqvist, K. Kainulainen, A. Sorri, JHEP 0104 (2001) 012.
- [38] K.S. Babu, I.Z. Rothstein, Phys. Lett. B285 (1992) 112;
L. Bento, Z. Berezhinani, Phys. Rev. D64 (2001) 115015.
- [39] L.D. Landau, Phys. Z. USSR 1 (1932) 426;
C. Zener, Proc. R. Soc. A 137 (1932) 696.
- [40] D.N. Spergel et al, astro-ph/0302209.

$\nu_\mu - \nu_s$ mixing – Non resonance case

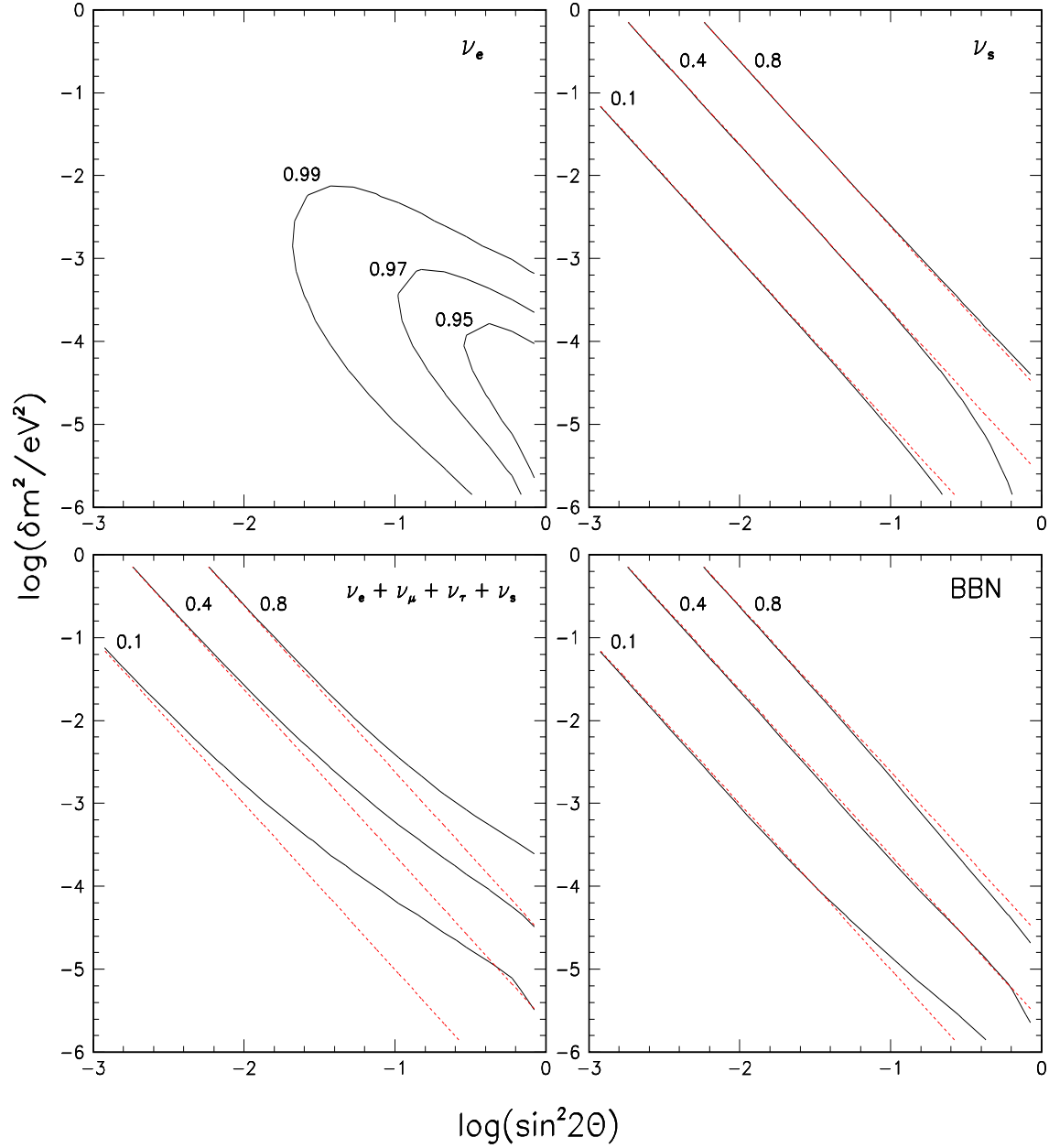


Figure 1: Numerical results for $\nu_\mu - \nu_s$ mixing. Non resonance case. *First panel:* Iso-countour lines for ν_e energy density. Each line corresponds to fixed value of ν_e energy density. The indicated values are normalized to equilibrium value. *Second panel:* Iso-countour lines for ν_s energy density. *Third panel:* Iso-countour lines for total neutrino contribution to the energy density. Each line corresponds to a fixed value of the number of extra neutrino flavors ΔN_ν . *Fourth panel:* Total effect of neutrino oscillation on BBN. Each line corresponds to a fixed value of the effective number of neutrinos $\Delta N_\nu^{\text{BBN}}$ species calculated according to eq. (28). Experimental bounds on $\Delta N_\nu^{\text{BBN}}$ exclude the region above the corresponding curve. Red dotted lines correspond to analytical estimates obtained from eq. (39) and following discussion. The quantities presented in this and in the following figures are taken at the BBN “time”, $x_{\text{BBN}} = 1.4$.

$\nu_e - \nu_s$ mixing – Non resonance case

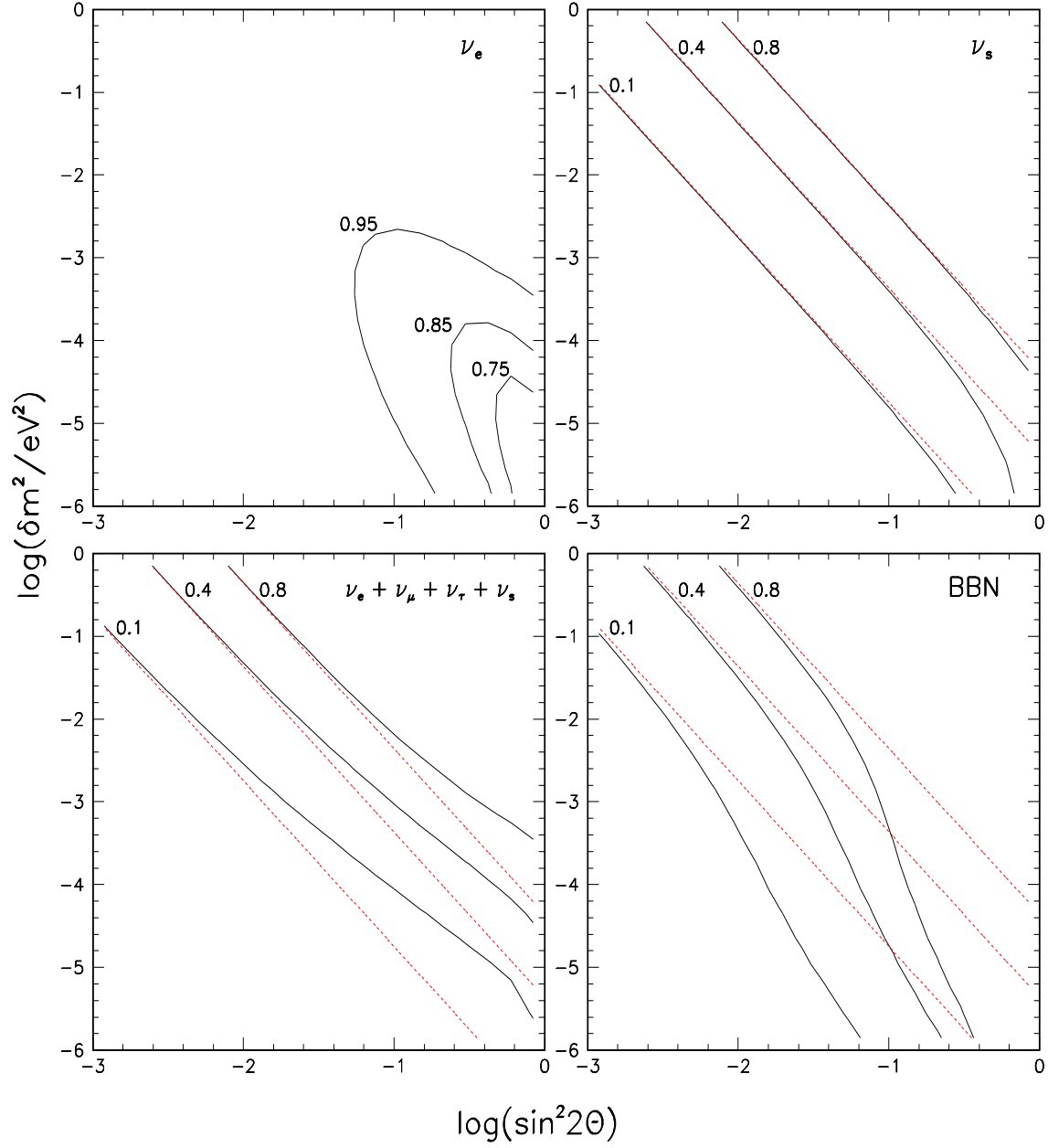


Figure 2: Numerical results for $\nu_e - \nu_s$ mixing, non resonance case. See Fig.1 for detailed explanation of the various panels and for a definition of the various lines. Red dotted lines correspond to analytical estimates obtained from eq.(38) and following discussion.

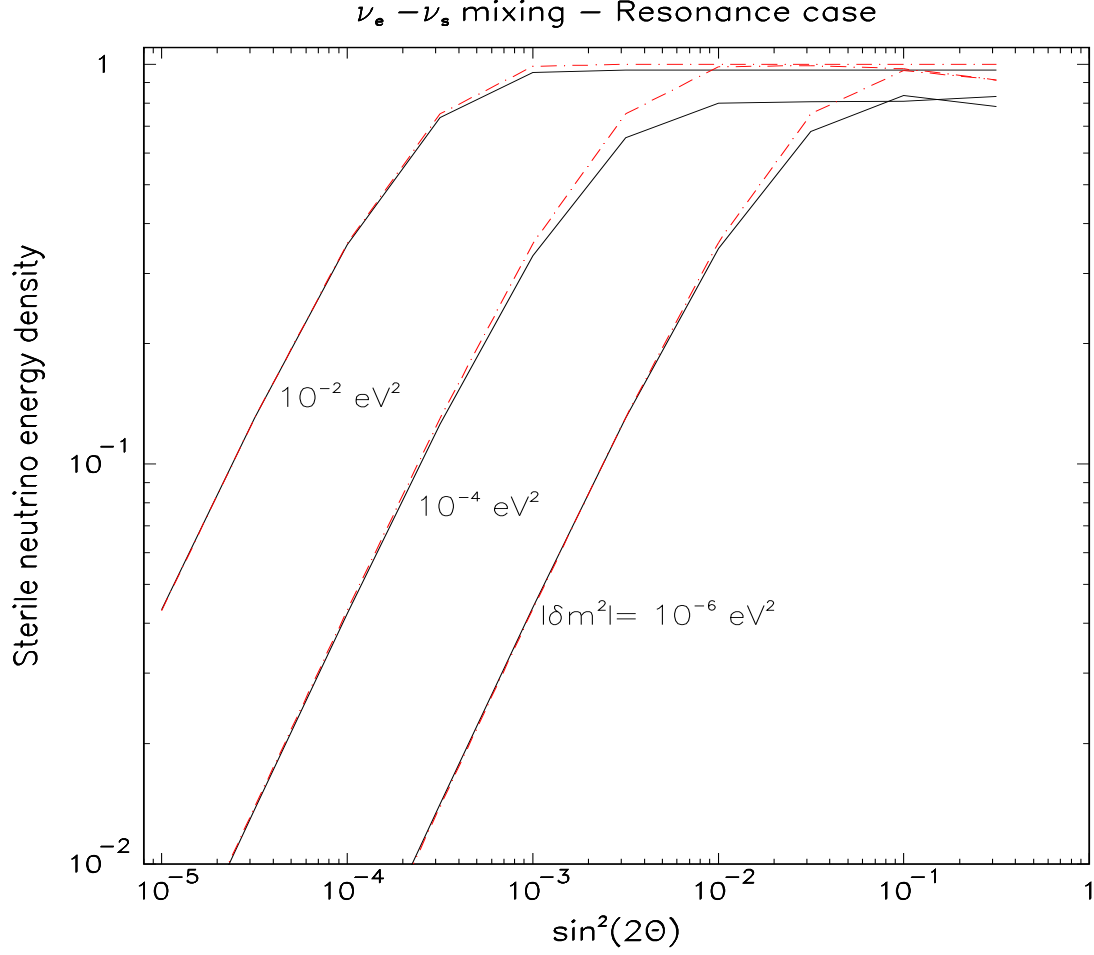


Figure 3: Comparison between numerical results (solid lines) and analytic estimates (red dotted lines) for $\nu_e - \nu_s$ mixing, resonance case. The various lines show the energy density of sterile neutrinos (at the time of BBN) as a function of the mixing angle $\sin^2(2\theta)$, for selected values of the mass difference δm^2 . Analytic estimates are obtained from eq. (57) and following discussion.

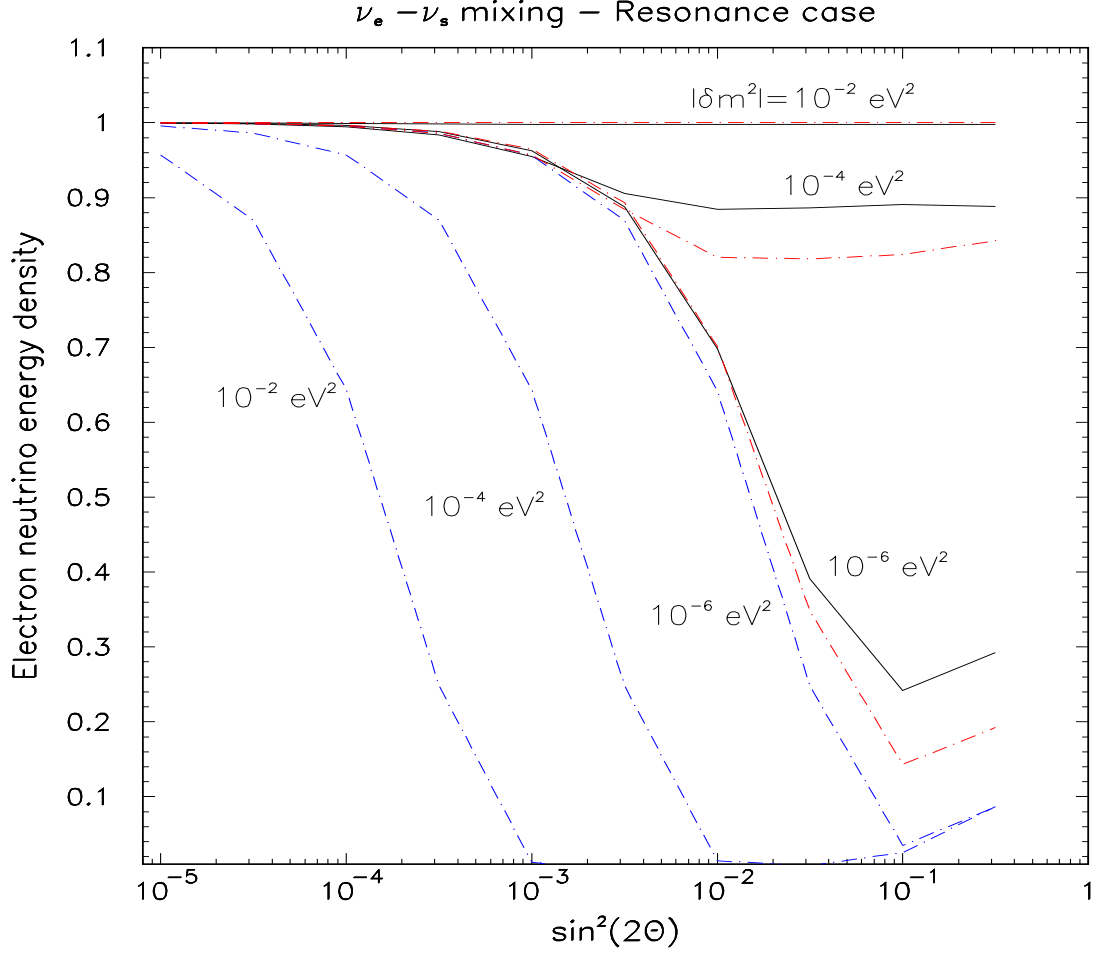


Figure 4: Comparison between numerical results (solid lines) and analytic estimates (dotted lines) for $\nu_e - \nu_s$ mixing, resonance case. The various lines show the energy density of electron neutrinos (at the time of BBN) as a function of the mixing angle $\sin^2(2\theta)$, for selected values of the mass difference δm^2 . Blue dotted lines, which are obtained from eqs. (56), do not take into account ν_e post-resonance evolution. Red dotted lines take it into account following eqs.(61, 62).

$\nu_\mu - \nu_s$ mixing – Resonance case

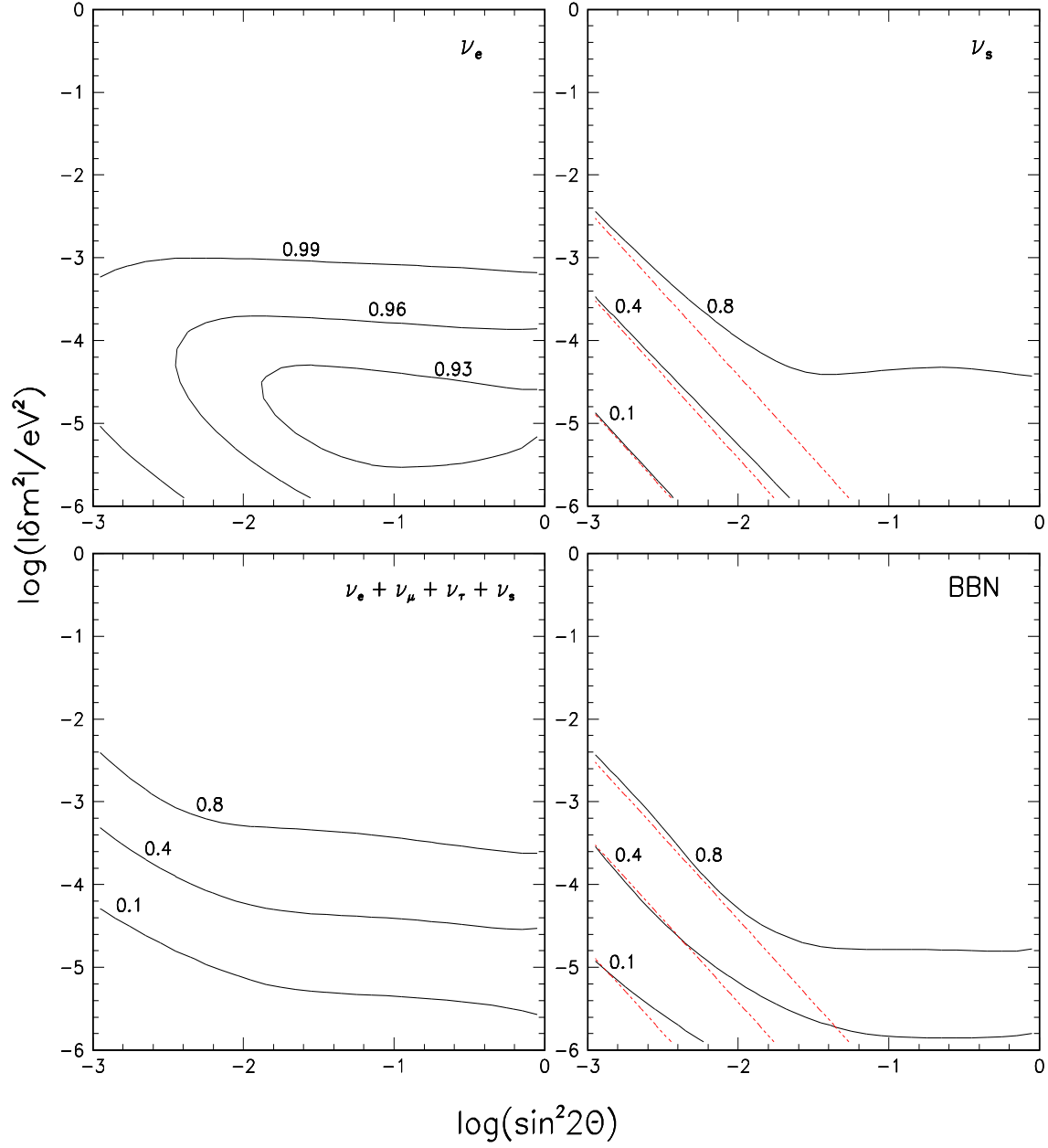


Figure 5: Numerical results for $\nu_\mu - \nu_s$ mixing, resonance case. See Fig.1 for detailed explanation of the various panels and for a definition of the various lines. Red dotted lines correspond to analytical estimates obtained from eq.(57) and following discussions.

$\nu_e - \nu_s$ mixing – Resonance case

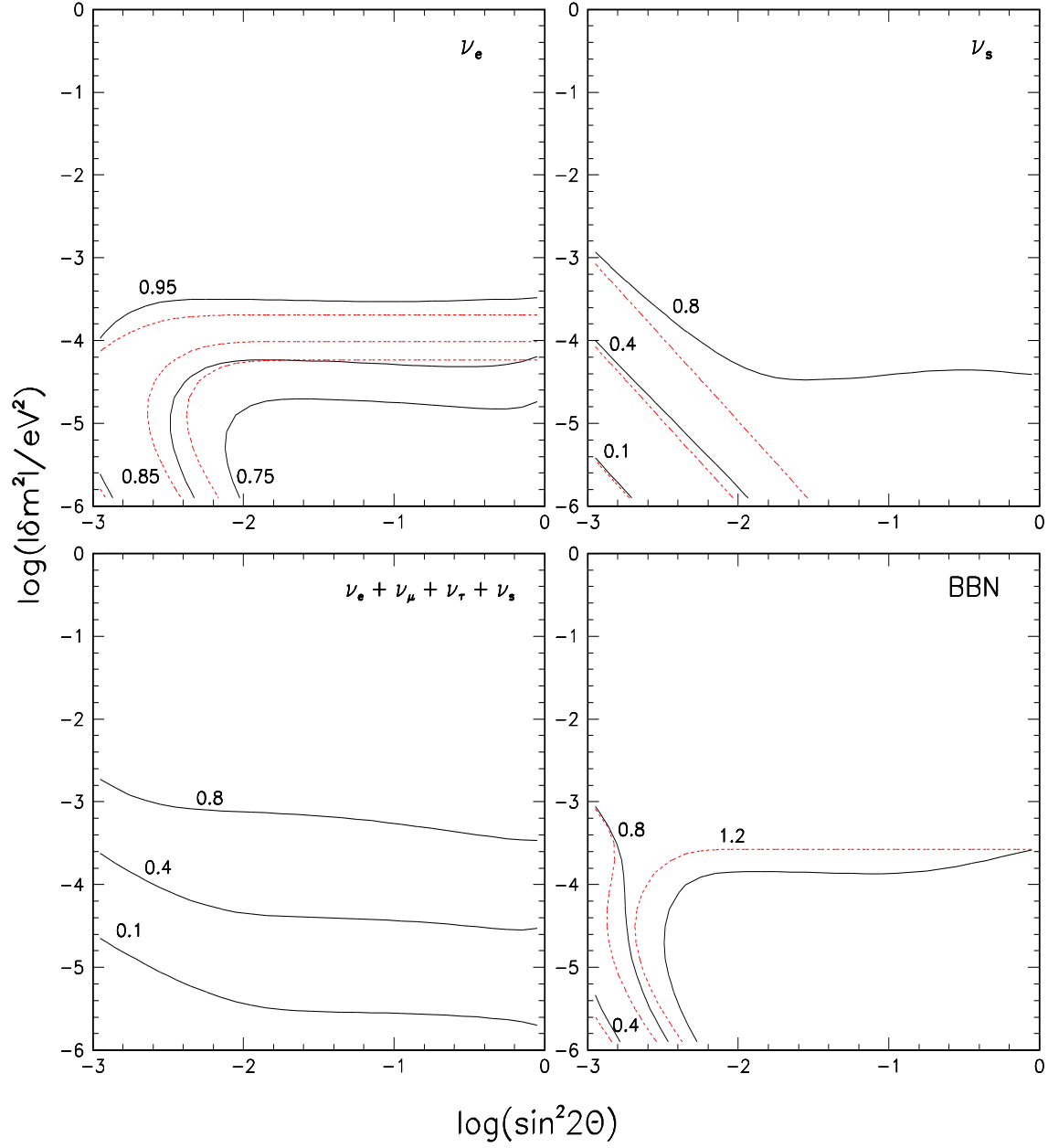


Figure 6: Numerical results for $\nu_e - \nu_s$ mixing, resonance case. See Fig.1 for detailed explanation of the various panels and for a definition of the various lines. Red dotted lines correspond to analytical estimates obtained from eq.(57) and following discussions.

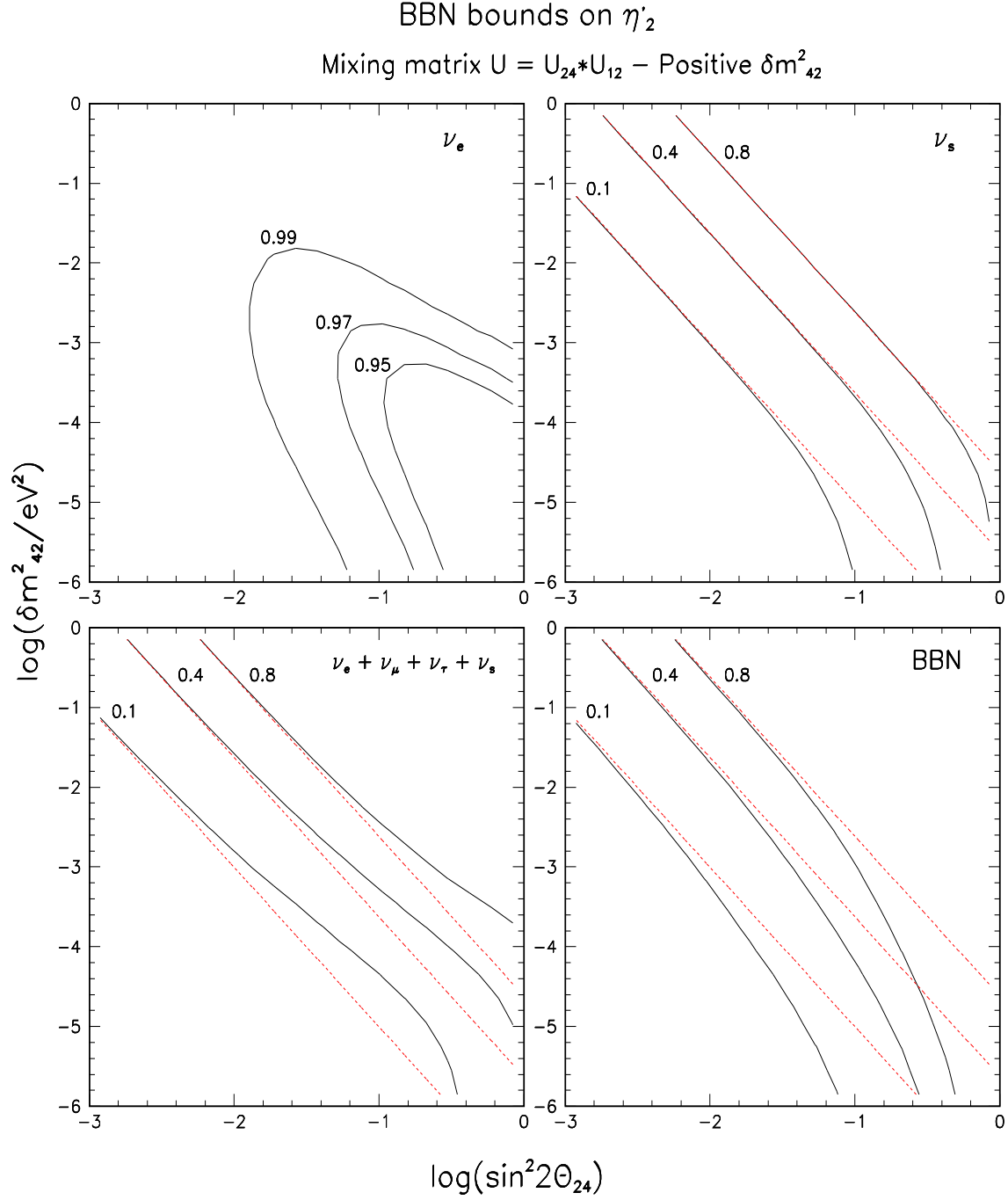


Figure 7: Numerical results for the case in which the neutrino mixing matrix can be written as $U = U_{24} \cdot U_{12}$, with δm^2_{21} and θ_{12} fixed according to eq. (1). We consider positive values for the mass difference $\delta m^2_{42} = m_4^2 - m_2^2$. See Fig.1 for a detailed explanations of the various panels and for a definition of the various lines. Red dotted lines correspond to analytic estimates obtained from eq.(97). Note that in the small mixing angle limits, the angle θ_{24} coincides with the parameter η'_2 defined in eq.(89)

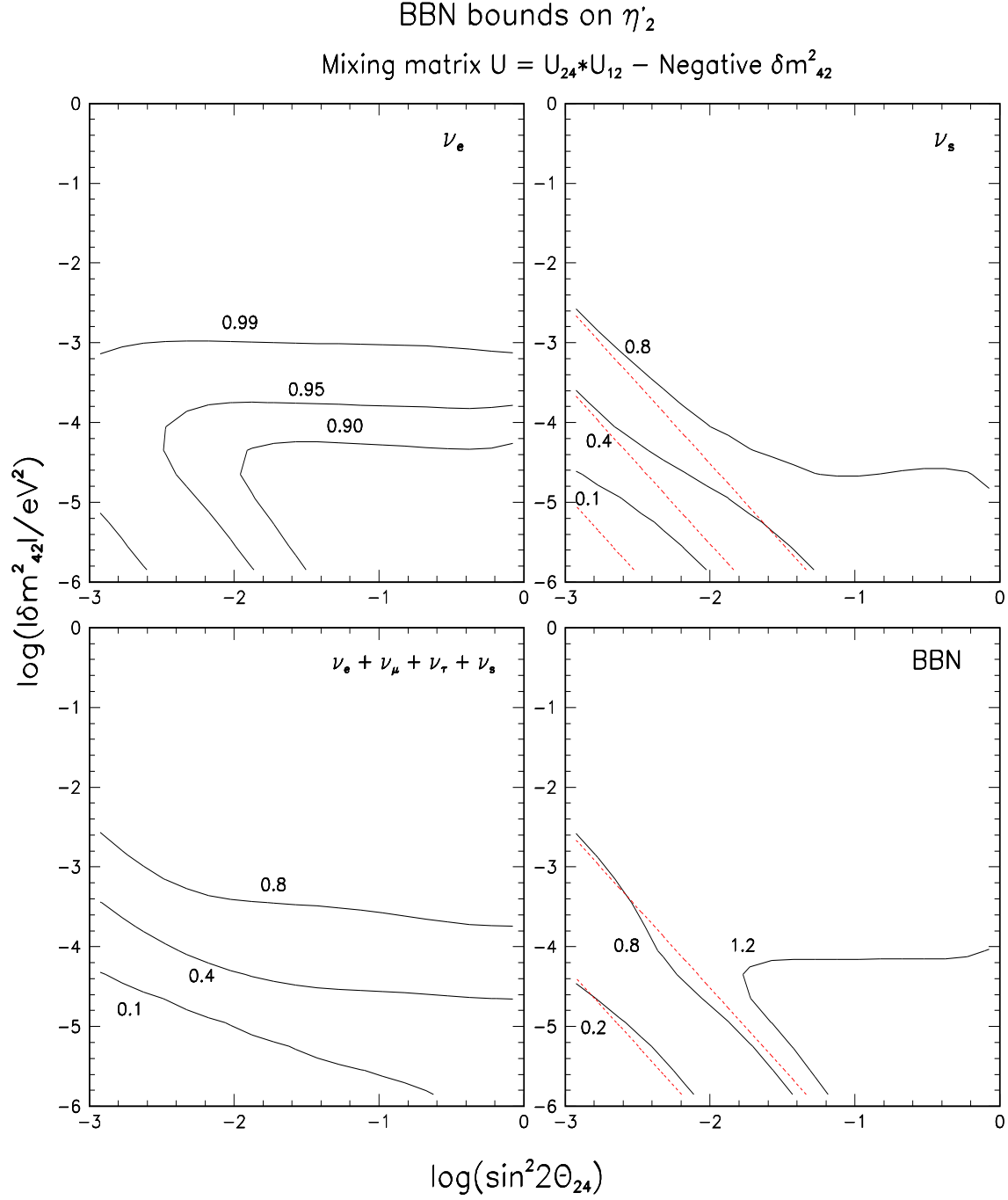


Figure 8: Numerical results for the case in which the neutrino mixing matrix can be written as $U = U_{24} \cdot U_{12}$, with δm_{21}^2 and θ_{12} fixed according to eq. (1). We consider negative values for the mass difference $\delta m_{42}^2 = m_4^2 - m_2^2$. See Fig.1 for detailed explanation of the various panels and for a definition of the various lines. Red dotted lines correspond to analytic estimates obtained from eq.(99). Note that in the small mixing angle limits, the angle θ_{24} coincides with the parameter η'_2 defined in eq.(89)

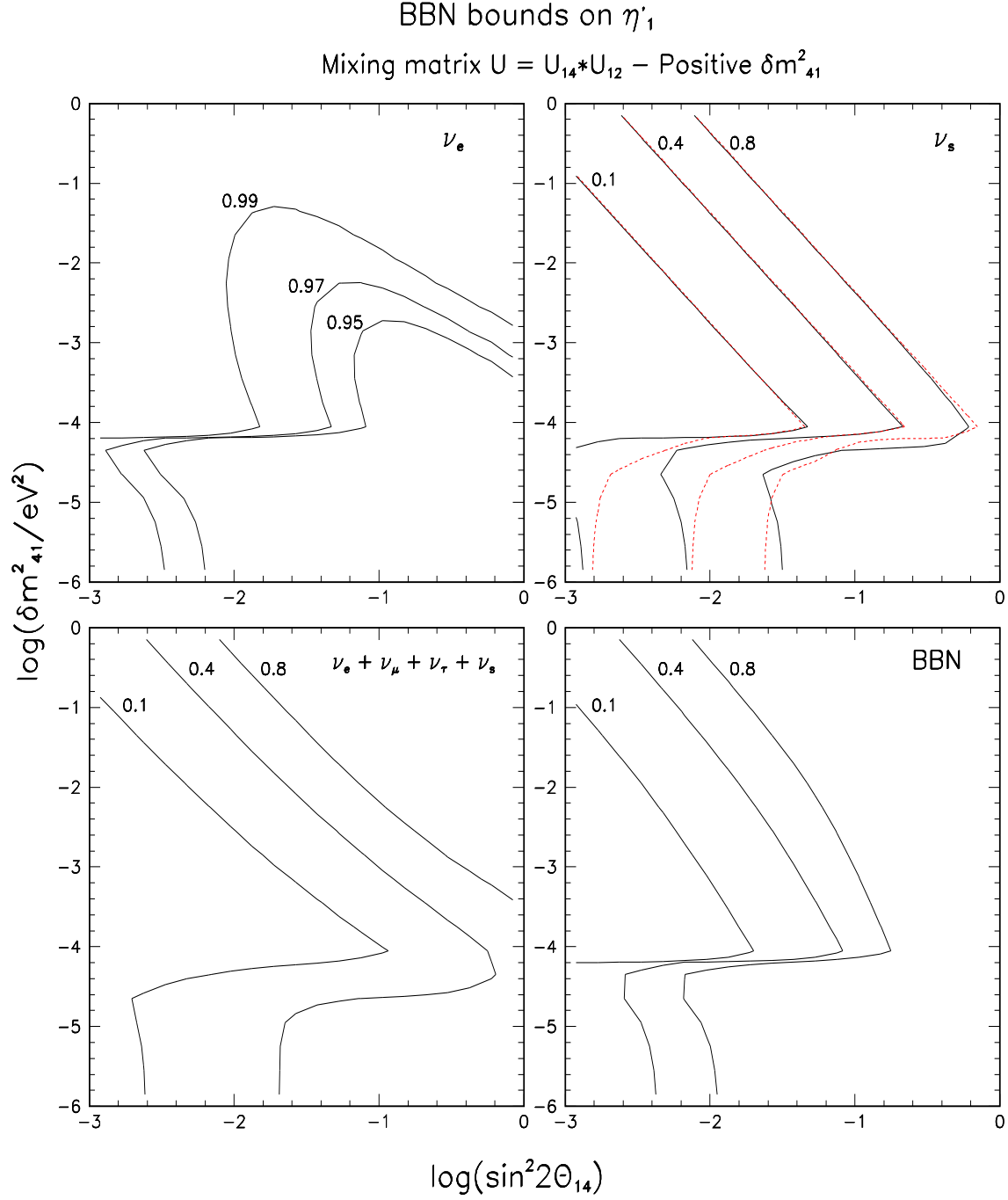


Figure 9: Numerical results for the case in which the neutrino mixing matrix can be written as $U = U_{14} \cdot U_{12}$, with δm^2_{21} and θ_{12} fixed according to eq. (1). We consider positive values for the mass difference $\delta m^2_{41} = m_4^2 - m_1^2$. See Fig.1 for detailed explanation of the various panels and for a definition of the various lines. Red dotted lines correspond to analytic estimates obtained from eqs.(96,102). Note that in the small mixing angle limits, the angle θ_{14} coincides with the parameter η'_1 defined in eq.(88)

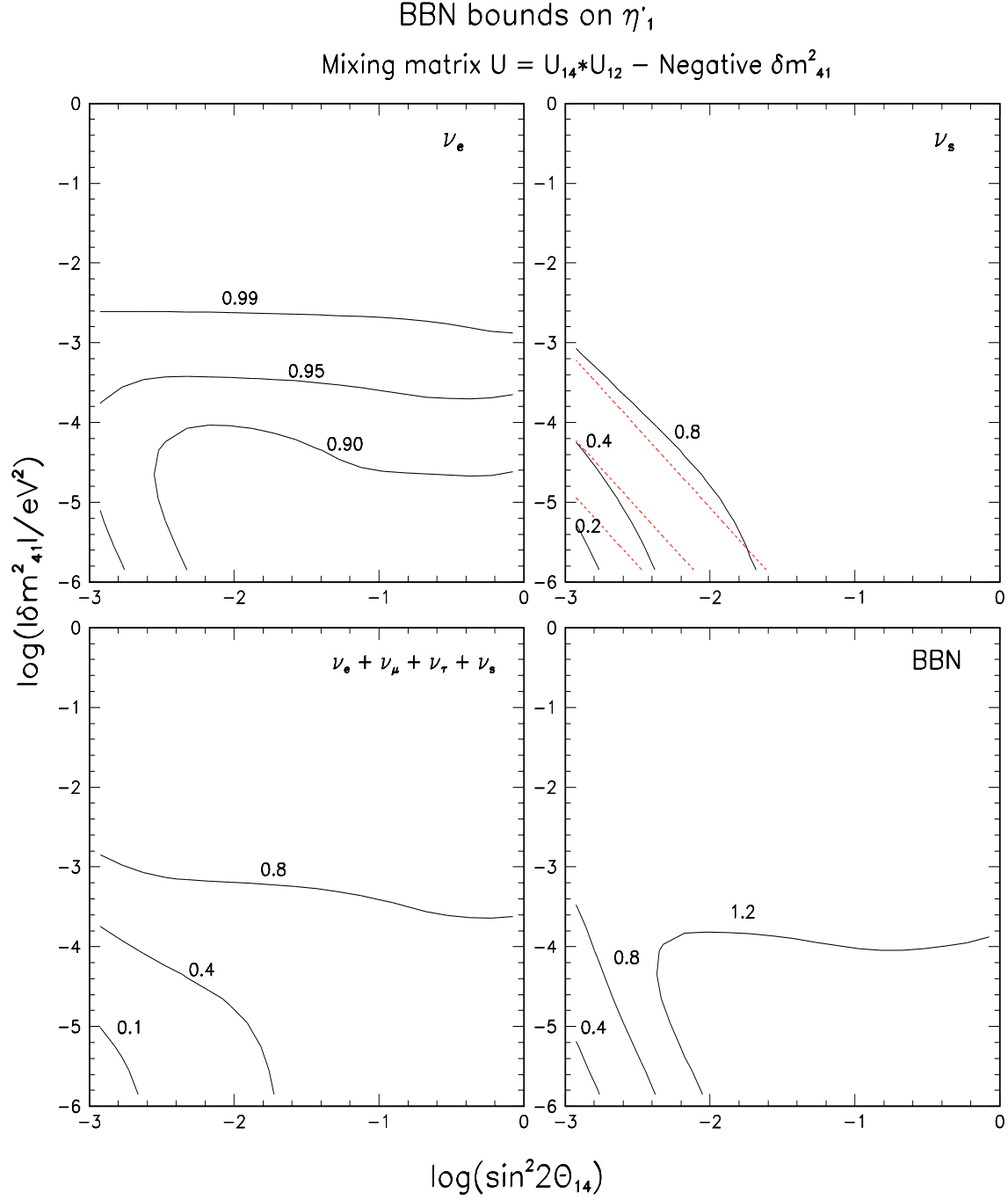


Figure 10: Numerical results for the case in which the neutrino mixing matrix can be written as $U = U_{14} \cdot U_{12}$, with δm^2_{21} and θ_{12} fixed according to eq. (1). We consider negative values for the mass difference $\delta m^2_{41} = m_4^2 - m_1^2$. See Fig.1 for detailed explanation of the various panels and for a definition of the various lines. Red dotted lines correspond to analytic estimates obtained from eq.(98). Note that in the small mixing angle limits, the angle θ_{14} coincides with the parameter η'_1 defined in eq.(88)